STUDIES OF STRUCTURAL, NONLINEAR OPTICAL AND THERMAL PROPERTIES OF SPECIFIC NONCONJUGATED CONDUCTIVE POLYMERS INCLUDING A CO-POLYMER STYRENE-BUTADIENE-RUBBER

by

Gurudutt Telang

A thesis submitted to the Graduate Faculty of
Auburn University
in partial fulfillment of the
requirements for the Degree of
Master of Science

Auburn, Alabama
August 4, 2012

Keywords: Nonconjugated conductive polymer, Styrene-butadiene-rubber, Photovoltaic, Quadratic Electro-optic effect, Differential Scanning Calorimeter

Approved by

Mrinal Thakur, Chair, Professor of Mechanical Engineering
Dan Marghitu, Professor of Mechanical Engineering
P K Raju, Thomas Walter Distinguished, Professor of Mechanical Engineering

Abstract

The structures, quadratic electro-optic effects, thermal properties, and photovoltaic characteristics of specific nonconjugated polymers have been studied. Various tools and techniques such as Optical absorption, Differential Scanning Calorimetry, and FTIR spectroscopy have been used to study these polymers, in particular a nonconjugated co-polymer styrene-butadiene-rubber (SBR). The optical absorption spectrum of styrene-butadiene-rubber at low doping of iodine showed two peaks at 4.27 eV and 3.2 eV due to radical cations and charge-transfer from double bond to dopant respectively. Upon doping, FTIR showed a reduction in the intensity of peaks 964 cm^{-1} and 910 cm^{-1} corresponding to =C-H bending vibration-band. This is due to transformation of double bonds into radical cation upon charge transfer.

Quadratic electro-optic effect for iodine doped styrene-butadiene-rubber has been measured at specific wavelengths 633 nm and 1550 nm using field-induced birefringence method. The Kerr coefficients measured at 633 nm and 1550 nm were $3.1x10^{-10}$ m/V^2 and $1.2x10^{-10}$ m/V^2 respectively. These Large Kerr coefficients and third order susceptibilities have been attributed to the subnanometer-size metallic domains (organic quantum dots) formed upon doping and charge-transfer.

Thermal properties of the specific nonconjugated conductive polymers have been studied over a range of temperatures (-55^0C to 110^0C) before and after doping with iodine. It was observed that specific heat capacity of poly(β-pinene) increases upon

doping while in the case of 1,4-trans-polyisoprene, SBR and cis-1,4-polyisoprene reduces. The T_g of undoped poly(β-pinene) as observed is at 77^0C and the T_m of 1,4-trans-polyisoprene has been found to be at 60^0C in this range respectively. After doping these thermal transitions were not clearly observable. In the case of styrene-butadiene-rubber and cis-1,4-polyisoprene, no significant change in heat flow characteristics and line-shape was found before and after doping with iodine.

The refractive indices of iodine doped poly(β-pinene) were calculated using Kramer-Kronig transformations utilizing the optical absorption data for high level of doping. Refractive indices at specific wavelengths (633nm) for doped PBP and SBR have been determined by measuring reflectivity at different angles of incidence. Photovoltaic effect in a composite involving nonconjugated conductive polymer, poly(β-pinene) (PBP) has been studied. Photovoltaic cells were constructed with iodine-doped poly(β-pinene) film sandwiched between two electrodes: 1) titanium dioxide on ITO glass and 2) carbon on ITO glass, and using potassium iodide as an electrolyte. It was observed that as the intensity of the incident light increases the photo-current and photo-voltage increases proportionally (photovoltaic effect).

Thus structural, optical, quadratic electro-optic effect, thermal properties and photovoltaic studies of specific nonconjugated conductive polymers including a novel co-polymer (Styrene-butadiene-rubber) have been made.

Acknowledgments

This work would not have been possible without the help, support and guidance of many close individuals. I take this opportunity first to express my gratitude to my advisor Dr. Mrinal Thakur who has not only guided in my research but also has been a great mentor to me throughout my study at the Auburn University. His suggestions and guidance from time to time has proved to be instrumental to this work. I am also very grateful to my committee members Dr. Maghitu and Dr. P K Raju for their valuable time and serving as my committee members.

Also, I am thankful to Photonic Research Material laboratory where I have spent most of the time for my research. I appreciate all the help from my colleagues Sapana Srivastava, Prashant Dubey and Mradul Sangal at Photonic Materials Research Laboratory. I am also thankful to all the lab instructors from various department labs for their instructions and help in my experiment that I conducted. I want to thank my Auburn friends (Vamsi, Rohan, Meetesh, Suryakant, Gopal), Mumbai University friends and colony friends for their encouragement and help during my masters. Finally, I thank my Mom, Dad, Purva, and rest of my family for their constant support and unconditional love.

Table of Contents

Abstract……..ii

Acknowledgments ……iv

List of Tables …….ix

List of Figures ……x

Chapter 1 INTRODUCTION……..1

Chapter 2 BACKGROUND…….5

2.1 Governing Maxwell's Equation ……....5

2.2 Interaction of light in an optical medium……..6

2.2.1 Isotropic medium 6

2.2.2 Anisotropic medium …….……...7

2.3.1 Linear optical processes …….…….8

2.3.2 Non Linear optical processes …….....9

2.3.2.1 Second order nonlinear processes ……..9

2.3.2.1.1 Sum-Frequency Generation……10

2.3.2.1 2 Difference-Frequency Generation …….……11

2.3.2.1 3 Second Harmonic Generation …….……...11

2.3.2.1 4 Third Harmonic Generation …….……..12

2.3.2.1 5 Optical Rectification Generation …….……..13

2.3.2.2 Third order nonlinear processes ……13

2.4 Nonlinear optical materials …….……15

2.4.1 Second order Optical Material …….……15

2.3.4.2 Third order Optical Material …….…16

2.5 Nonconjugated conducting polymers (NCP) …….……17

2.6 FTIR Spectroscopy ……18

2.7 Electro-Optic Effect …….……...19

2.8 Differential Scanning Calorimetry (DSC)……...22

2.8 Refractive index……...23

2.8.1 Kramers- Kronig Relations in Nonlinear optics……26

Chapter 3 OBJECTIVES……...27

Chapter 4 NONCONJUGATED CONDUCTIVE POLYMERS……..29

4.1 Poly (ß-pinene) (PBP)…….30

4.2 Polyisoprene …….....31

4.2.1 Trans-1,4-polyisoprene (TPI) ……..31

4.2.2 Cis-1,4-polyisoprene (CPI)……...32

4.3 Styrene-butadiene-rubber (SBR)…….33

Chapter 5 COMPARISON OF OPTICAL PROPERTIES OF NANOMETALLIC AND DOPED NONCONJUGATED CONDUCTIVE POLYMERS…….34

5.1 Introduction……..……34

5.2 Nonlinear optical properties.....…...35

5.3 Comparison of Third order Optical Nonlinearities……..…36

Chapter 6 QUADRATIC ELECTRO- OPTIC EFFECT AND STRUCTURAL STUDIES OF NONCONJUGATED CO-POLYMER STYRENE-BUTADIENE-RUBBER……...38

6.1 Introduction……..38

6.2 Optical absorption……39

6.3 FTIR Measurements……41

6.4 Sample preparation for Electro-optics experiment……..42

6.5 Experimental Setup ……43

6.6 Result and Discussion……..44

6.7 Conclusion……...48

Chapter 7 STUDIES OF THERMAL PROPERTIES IN NONCONJUGATED POLYMERS USING DIFFERENTIAL SCANNING CALORIMETRY (DSC).....49

7.1 Introduction……..49

7.2 Specific heat of Nano particles…….....49

7.3 Differential Scanning Calorimetry (DSC)……...50

7.4 Experiment……...51

7.5 Results……..52

7.5.1 DSC of trans-1,4-polyisoprene……..52

7.5.2 DSC of Poly(β-pinene) ……55

7.5.3 DSC of Styrene-Butadiene-Rubber …….……..57

7.5.4 DSC of Cis-1,4-polyisoprene…….……60

7.6 Discussion……62

7.7 Conclusion……...64

Chapter 8 PHOTOVOLTAIC EFFECT IN A COMPOSITE INVOLVING IODINE-DOPED POLY(β-PINENE), A NONCONJUGATED CONDUCTIVE POLYMER.....73

8.1 Introduction…….....66

8.2 Experiment……...68

8.3 Result and Discussions……69

8.4 Conclusion……...71

Chapter 9 STUDY OF ABSORPTION COEFFICIENT AND REFRACTIVE INDICES OF NONCONJUGATED POLYMERS USING SPECIFIC METHODS……....72

9.1 Introduction…….72

9.2 Result and Discussions……72

9.3 Conclusion……...77

Chapter 10 SUMMARY……79

BIBLIOGRAPHY……..81

List of Tables

Table 5.1 Third order nonlinear properties of nanoparticle and polymers……....37

Table 6.1 Comparison of third order nonlinearities……...47

Table 7.1 Specific heat capacities of specific NCP before and after iodine doping……..64

Table 9.1 Refractive indices for different incident angles for PBP……...76

Table 9.2 Refractive indices for different incident angles for SBR……...77

Table 9.2 Refractive indices of iodine doped SBR at 633 nm for specific methods.....77

List of Figures

Figure 2.1: Sum-Frequency Generation……...11

Figure 2.2: Difference of Frequency Generation…….11

Figure 2.3: Second-harmonic Generation ……...12

Figure 2.4: DSC plot of heat flow vs. temperature in a material ……22

Figure 2.5: Refractive index and Absorption coefficient of fused silica ……25

Figure 4.1: Molecular structure of poly(β-pinene) ……..30

Figure 4.2: Molecular structure of trans-1, 4- polyisoprene……31

Figure 4.3: Micrograph of trans-1,4- polyisoprene film …….32

Figure 4.4: Molecular structure of cis-1,4-polyisoprene ……32

Figure 4.5: Molecular structure of styrene-butadiene-rubber …….33

Figure 5.1 Absorption spectra of Gold nanoparticle of different diameter …….……35

Figure 5.2: Third order susceptibility of gold nanoparticles ……...36

Figure 6.1: Transformation of double bond into cation radicals in SBR ……39

Figure 6.2: Optical absorption of styrene-butadiene-rubber …….……..40

Figure 6.3: Optical Absorption of Silver Nanocrystal ……41

Figure 6.4 FTIR spectroscopy of styrene-butadiene-rubber …….……..42

Figure 6.5: Molecular structure of undoped styrene-butadiene-rubber …..……43

Figure 6.6: Experimental setup for electro-optics ……...44

Figure 6.7: Quadratic modulation depth due to applied Electric field for 633nm …..44

Figure 6.8: Quadratic modulation depth due to applied Electric field for 1550 nm ...45

Figure 7.1: DSC plot of heat flow vs. temperature in a material ……51

Figure 7.2: DSC scan of trans-polyisorene before doping ……..53

Figure 7.3: DSC scan of trans-polyisoprene after doping ……...53

Figure 7.4: DSC scan of trans-polyisoprene before doping (0^0C to 30^0C) …….54

Figure 7.5: DSC scan of trans-polyisoprene after doping (0^0C to 30^0C) ……54

Figure 7.6: DSC scan of poly(β-pinene) before doping ……..55

Figure 7.7: DSC scan of poly(β-pinene) after doping ……56

Figure 7.8: DSC scan of poly(β-pinene) before doping for range (0^0C to 25^0C) …....56

Figure 7.9: DSC scan of poly(β-pinene) after doping for range (0^0C to 25^0C) ……..57

Figure 7.10: DSC scan of styrene-butadiene rubber before doping ……58

Figure 7.11: DSC scan of styrene-butadiene rubber after doping ……...58

Figure 7.12: DSC scan of SBR before doping for the range (25^0C to 35^0C) ……..59

Figure 7.13: DSC scan of SBR after doping for the range (25^0C to 35^0C) …….59

Figure 7.14: DSC scan of cis-1,4-polyisoprene before doping ……...60

Figure 7.15: DSC scan of cis-1,4-polyisoprene after doping ……..61

Figure 7.16: DSC scan of undoped CIS before doping for range (20^0C to 35^0C) …..61

Figure 7.17: DSC scan of undoped CIS before doping for range (20^0C to 35^0C)…...62

Figure 8.1: World Population statistics ……...67

Figure 8.2: World Energy Consumption from 1980-2030 ……..67

Figure 8.3: Experimental setup for photovoltaic ……....69

Figure 8.4: Plot of Intensity vs. Photo-Voltage ……..69

Figure 8.5: Plot of Intensity vs. Photo-Current……...70

Figure 9.1: Absorption coefficient SBR at heavy doping with iodine……74

Figure 9.2: Refractive index of heavily poly(β-pinene) ……..75

Chapter 1

INTRODUCTION

Photonics is one of the fastest growing fields of science and technologies in the modern world. It blends together optics and electronics to effectively handle and process enormous amount of data with exceptional speed. Photonic science has wide range of applications that include generation, emission, signal processing, transmission, switching, amplification, detection and sensing of light. Also photonics finds its application in numerous fields including telecommunication, medical science, optics, electronics etc. Continued research on linear and nonlinear optical properties of materials builds the core of such applications in photonics. Novel nanomaterials and structure provide immense scope to the field of photonic applications. This presented thesis deals with research performed on new organic nanometallic materials.

At present, scientists and technologists are exploring new types of renewable resources i.e. wind energy, geothermal energy, bio-fuel, solar energy etc. The need for exploring these renewable resources is due to the increasing consumption of nonrenewable energy resources. Renewable source device such as solar cell is used to convert incident light energy into electrical energy. These cells are generally made of some inorganic and organic materials, which absorb light from the source, release electrons and produce electricity. Inorganic materials have been the

main ingredient of photovoltaic cell for few decades, but its fabrication and installation is costly. Due to these drawbacks of inorganic materials, organic material got much into attention of photonic researchers. Low dielectric property and high optical property not only makes them applicable in photovoltaic cell but also used in many other application of photonics, i.e. electro-optics, absorption etc.

In this jet age, we deal with enormous amount of data processing at exceptionally high speed. As a result it has generated a considerable amount of interest among researchers to explore these organic materials like nonconjugated conductive polymers in the communication field. Their low dielectric constants ensure that the speed is never compromised. Further ease of fabrications and the flexibility they provide to the engineer at molecular level have made them very popular. Hence it would not be surprising, if these materials soon become the backbone of the optical communication, information storage and other important fields. As a result exploring the basic nonlinear properties of such novel materials is must. But much waits to be explored and experiment in this field. The research discussed is divided into the following areas:

1. Quadratic electro-optics effect of nonconjugated conductive co-polymer styrene-butadiene-rubber , doped with iodine at shorter wavelength
2. Thermal properties of specific nonconjugated conductive polymers poly(β-pinene) (PBP), trans-1,4-polyisoprene (TPI), cis-1,4-polyisoprene (CIS) and a co-polymer styrene-butadiene-rubber (SBR) by using Differential Scanning Calorimeter, before and after doping with iodine.
3. Photovoltaic effect in a composite involving nonconjugated conductive polymer, poly(β-pinene) (PBP).

4. Refractive indices of iodine doped nonconjugated co-polymer styrene-butadiene-rubber (SBR) and poly(β-pinene) using Kramer-Kronig transformation and determination of refractive index for different angle of incidence.

The research work is systematically organized into chapters with an appropriate sequence.

Chapter 1: Consist of an introduction to the thesis research work.

Chapter 2: titled "Background" explains the basic theories and fundamental concepts of photonic and nonlinear optics and properties, that support the proposed thesis.

Chapter 3: Overall goals of this research and studies are discussed in this chapter, titled as "Objective".

Chapter 4: Discusses the physical structure and electrical properties of nonconjugated conductive polymers.

Chapter 5: Optical nonlinear properties of various nanomaterials and metal nanoparticles are explained and compared with optical properties of nonconjugated conductive co-polymer styrene-butadiene-rubber in this chapter.

Chapter 6: Describes the quadratic electro-optic effect in the nonconjugated conductive co-polymer iodine-doped styrene-butadiene-rubber measured at specific wavelength 633 nm and 1550 nm.

Chapter 7: Explains the thermal properties on specific nonconjugated conductive polymers before and after doping. This study of characterization of the specific nonconjugated polymer is done by differential scanning calorimetry.

Chapter 8: Discusses the photovoltaic effect in a composite involving nonconjugated conductive polymer, poly(β-pinene) (PBP).

Chapter 9: Studies the refractive index of nonconjugated polymers using Kramer-Kronig transformation.

Chapter 10: Summarizes the proposed research work.

Chapter 2

BACKGROUND

In recent years, there has been a rapid expansion of activities in the field of nonlinear optics. Nonlinear optics is the study of phenomena that occurs due to modification of the optical properties of a medium in the presence of an electric field or an intense laser light. Some of these nonlinear responses includes: linear and quadratic electro-optic modulation/switching, optical limiting, frequency conversion, all-optical modulation, and others [1-4].

2.1 Governing Maxwell's Equation

The theory of propagation of light was first proposed by James Clerk Maxwell and was later confirmed by Heinrich Hertz [5, 6]. Light travels as an electromagnetic wave for which the direction of propagation, magnetic field and electric field are mutually perpendicular to each other. The propagation of light is governed by Maxwell's equations. Maxwell's equations describe classical optics and electrodynamics using a set of partial differential equations. The Maxwell's equations for electric and magnetic field vectors $\vec{E}$ and $\vec{H}$ and $\vec{B}$ and $\vec{D}$ as electric and magnetic displacement vectors is established using following equations. [7, 8]

$$\nabla . \vec{D} = \rho \qquad \text{Eqn. (2.1)}$$

$$\nabla . \vec{B} = 0 \qquad \text{Eqn. (2.2)}$$

$$\nabla \times \vec{E} = -\frac{\partial \vec{B}}{\partial t} \qquad \text{Eqn. (2.3)}$$

$$\nabla \times \vec{\mathrm{H}} = \mathrm{J} + \frac{\partial \overrightarrow{\mathrm{D}}}{\partial \mathrm{t}} \qquad \text{Eqn. (2.4)}$$

Where ρ and *J* stands for electric charge and current densities respectively.In optics, for most cases, one deals with negligible electrical or thermal conductivity referred as dielectric. This causes no free charge and no current (Conductivity is defined by the flow of electric charges) resulting into ρ and *J* to be zero. When electromagnetic field is applied, there is a possible atomic orbital distortion which is described as polarization magnetization. The effect of electromagnetic field on material media is governed by these equations

$$\vec{B} = \mu_0\left(\vec{\mathrm{H}} + \vec{\mathrm{M}}\right) \qquad Eqn.(2.5)$$

$$\vec{D} = \varepsilon_0 \vec{E} + \vec{P} \qquad Eqn.(2.6)$$

ε and μ are permittivity tensor and permeability tensor and $\vec{\mathrm{P}}$ and $\vec{\mathrm{M}}$ are electric and magnetic polarizations respectively. The ε_0 and μ_0 are permittivity and permeability of vacuum respectively.

2.2 Interaction of light in an optical medium

Optical media can be classified into two types:

1. Isotropic medium

2. Anisotropic medium

2.2.1 Isotropic medium

The term ‘isotropy’ refers to having similar properties for all direction in a medium. The electric field $\vec{E}$, displacement vector $\vec{D}$ and polarization $\vec{P}$ do not depend on the direction of electric field in an isotropic medium. The polarization induced is always parallel to applied electric field; it always carries a linear relationship. Thus linear polarization for an isotropic medium is expressed by the following equation.

$$\vec{P} = \varepsilon_0 \chi \vec{\mathrm{E}} \qquad Eqn(2.7)$$

Correspondingly, the relationship between the displacement vector and the susceptibility χ is given by

$$\vec{D} = \varepsilon_0 (1 + \chi) \vec{\mathrm{E}} \qquad Eqn(2.8)$$

In an isotropic medium electrons are tightly bound to the nucleus, which makes these materials non-conducting and nonmagnetic. As a result these materials can be compared to the dielectric medium when subjected to an external electric field. The polarization due to the dipole, induced by the electric field is mention below [2].

$$P = -Ner \qquad Eqn.(2.9)$$

Where *P* is the polarization, e is the electronic charge, and *r* is the displacement induced by the electric field. Correspondingly the wave equation for such a medium can be stated as

$$\nabla \times \nabla \times \vec{E} = \nabla \times (-\frac{\partial \vec{\mathrm{B}}}{\partial \mathrm{t}}) \qquad Eqn(2.10)$$

2.2.2 Anisotropic medium

The term 'anisotropy' refers to different properties for different directions in a media. In this directionally dependent nonlinear medium, the polarization is not necessarily parallel to the applied electric field. And hence the polarization *P* can be expressed by the following equations given below.

$$P_1 = \varepsilon_0 \left(\chi_{11} E_1 + \chi_{12} E_2 + \chi_{13} E_3 \right) \qquad Eqn.(2.11)$$

$$P_2 = \varepsilon_0 \left(\chi_{21} E_1 + \chi_{22} E_2 + \chi_{23} E_3 \right) \qquad Eqn.(2.12)$$

$$P_3 = \varepsilon_0 \left(\chi_{31} E_1 + \chi_{32} E_2 + \chi_{33} E_3 \right) \qquad Eqn.(2.13)$$

Where χ the susceptibility is a tensor of rank 2 and the electric displacement vector *D* is given by

$$D_i = \varepsilon_i (1 + \chi_{ij}) E_i = \varepsilon_{ij} E_j \qquad (2.14)$$

where ε_{ij} represents the permittivity tensor. If a co-ordinate system is chosen such that it coincides with the principal dielectric axes of the medium, we get the following matrices.

$$\begin{bmatrix} D_x \\ D_y \\ D_z \end{bmatrix} = \begin{bmatrix} \varepsilon_x & 0 & 0 \\ 0 & \varepsilon_y & 0 \\ 0 & 0 & \varepsilon_z \end{bmatrix} \begin{bmatrix} E_x \\ E_y \\ E_z \end{bmatrix} \qquad (2.15)$$

The energy density due to the electric field is given by

$$U = \frac{1}{2} D.E \qquad (2.16)$$

Since the x, y, z are chosen along the principal axes, we have

$$U = \frac{1}{2} [\varepsilon_{11} E_1^2 + \varepsilon_{22} E_2^2 + \varepsilon_{33} E_3^2] \qquad (2.17)$$

$$2U = \frac{D_1^2}{\varepsilon_{11}} + \frac{D_2^2}{\varepsilon_{22}} + \frac{D_3^2}{\varepsilon_{33}} \qquad (2.18)$$

If $x = D_1\sqrt{2U}$, $y = D_2\sqrt{2U}$, $z = D_3\sqrt{2U}$ (2.19)

$$\frac{x^2}{n_x^2} + \frac{y^2}{n_y^2} + \frac{z^2}{n_z^2} = 1 \qquad (2.20)$$

Equation (2.20) is known as the indicatrix equation, it shows the relationship between the refractive index and the direction of polarization in a nonlinear anisotropic medium. Since the indicatrix equation traces the path of an ellipsoid, it is also referred to as refractive index ellipsoid [9].

2.3.1 Linear optical processes

Before the introduction of lasers, optical phenomenon was considered to be linear. The relationship between the polarization and the electric field was considered to be linear. The electric field and linear polarization are expressed as

$$\vec{E}(\vec{r}, t) = \vec{E}_0 \exp(\vec{k} . \vec{r} - \omega . t) + c.c \qquad Eqn. (2.21)$$

$$\vec{P} = \varepsilon_0 \chi^{(1)} \vec{E} \qquad Eqn. (2.22)$$

And the real dielectric constant is expressed as

$$\varepsilon = 1 + \chi^{(1)} = \{n + i\alpha\frac{c}{2\omega}\}^2 \qquad Eqn.(2.23)$$

Where n is refractive index, α is absorption coefficient and $\chi^{(1)}$ is linear susceptibilities respectively.

2.3.2 Nonlinear optical processes

It was observed that with the advent of lasers linear relationship did not hold good. A nonlinear dependence of polarization with applied electric field was reported [8-12]. In nonlinear optical media, the propagation of light is not so simple. The polarization depends on higher powers of electric field and is usually highly anisotropic. In an isotropic dielectric media; polarization occurs due to applied electric field, while in anisotropic media it may not be.

$$\vec{P} = \varepsilon_0(\chi^{(1)}\vec{E}(t) + \chi^{(2)}\vec{E}^2(t) + \chi^{(3)}\vec{E}^3(t) + \chi^{(4)}\vec{E}^4(t) + \cdots) \qquad Eqn.(2.24)$$

$$\vec{P} = \vec{P}^{(1)}(t) + \vec{P}^{(2)}(t) + \vec{P}^{(3)}(t) + \cdots \qquad Eqn.\ (2.25)$$

Where $\chi^{(2)}$ and $\chi^{(3)}$ are second and third order susceptibilities, and $\vec{P}_L$ and $\overrightarrow{P_{NL}}$ represents linear and nonlinear polarization respectively.

$$\vec{P}_L = \vec{P}^{(1)}(t) \quad Eqn.(2.26)$$

$$\overrightarrow{P_{NL}} = \varepsilon_0\left(\chi^{(2)}\vec{E}^2(t) + \chi^{(3)}\vec{E}^3(t) + \chi^{(4)}\vec{E}^4(t) + \cdots\right) \qquad Eqn.(2.27)$$

$$\vec{P} + \overrightarrow{P_{NL}} = \varepsilon_0(\chi^{(1)}\vec{E}(t)\varepsilon_0\left(\chi^{(2)}\vec{E}^2(t) + \chi^{(3)}\vec{E}^3(t) + \chi^{(4)}\vec{E}^4(t) + ..\right) Eqn.(2.28)$$

2.3.2.1 Second order nonlinear processes

Nonlinear optical materials can be classified as centrosymmetric and non centrosymmetric. Centrosymmetric materials are those materials in which polarization is an odd function of electric field. Since P (-E) = -P (E) holds well in centrosymmetric materials, the even terms are zero. In centrosymmetric materials

$$\chi^{(2)}E_2 = -\chi^{(2)}E_2 \qquad (2.29)$$

This is possible only when $\chi^{(2)} = 0$ or $\chi^{(2n)} = 0$ for all positive integers of n.

Whereas non-centrosymmetric materials are those materials in which polarization is an even function of electric field. Since P (-E) is not equal to P (E) in non-centrosymmetric materials, the even terms can be nonzero. Clearly it is seen that the optical material should be non-centrosymmetric to exhibit second order nonlinear properties.

Nonlinear optics gives rise to a host of optical phenomena. Discusses below are few second order nonlinear properties. These are as follows.

1. Sum frequency generation, Second harmonic generation
2. Difference frequency generation
3. Third harmonic generation
4. Optical rectification

2.3.2.1.1 Sum-Frequency Generation

Sum frequency generation is a nonlinear optical process used to study the molecular structure and dynamics at the surface and interfaces. When in a strong applied field, two laser beams having strong frequency ω_1 and a weak applied field frequency ω_2 interact with nonlinear material; there is a situation in which the strong signal ω_1, combine with the weak signal ω_2 to produced higher frequency signal $\omega_3 = \omega_1 + \omega_2$ [7].

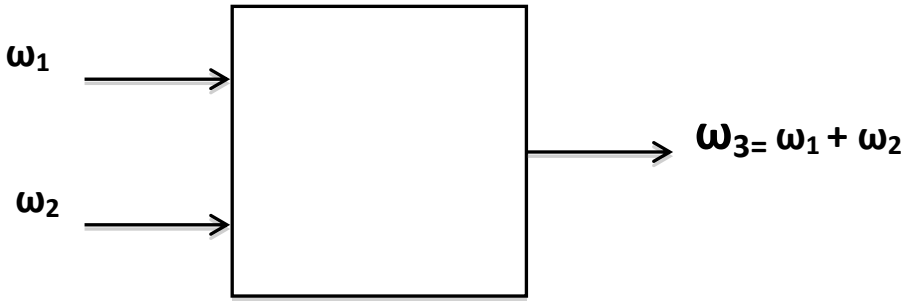

Figure 2.1: Sum-Frequency Generation

2.3.2.1.2 Difference-Frequency Generation

In this process, applied input fields with input frequencies ω_1 or ω_2 and ω_3 interact with nonlinear medium to produce output frequency as the difference between the other two frequencies. This process is similar to sum of frequency process. However in this processes, applied input fields (with frequencies ω_1 or ω_2 and ω_3) interact with lossless nonlinear material to produce an output signal at difference frequency ($\omega_2 = \omega_3 - \omega_1$) or ($\omega_1 = \omega_3 - \omega_2$).

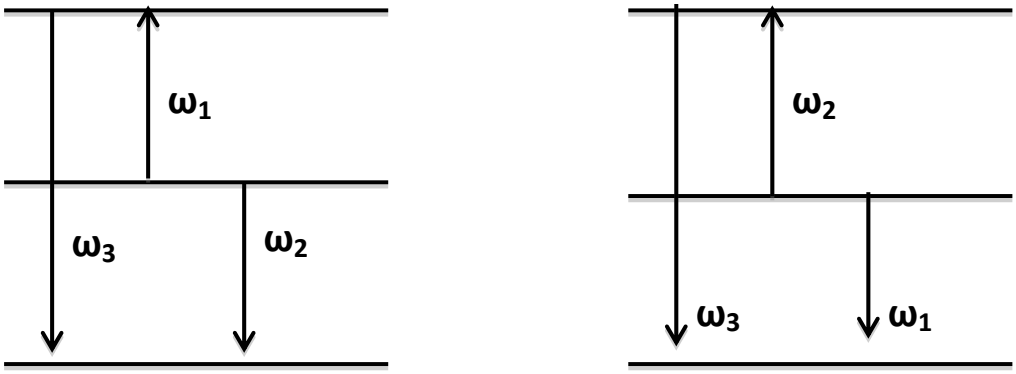

Figure 2.2: Difference of Frequency Generation

2.3.2.1.3 Second harmonic Generation

Second harmonic generation (SHG) is also denoted as frequency doubling. It is a nonlinear optical process in which photons interact with a nonlinear material, merging effectively to form new photons with twice the energy, and therefore twice the frequency and half the wavelength of the input photons. Second harmonic

generation is regarded as a specialcase of sum frequency generation. Full permutation symmetry of susceptibilities have been seen in second harmonic generation which are primarily caused by two fundamental frequencies ω_1 and $\omega_2 = 2\omega_1$. The $\omega_2 = 2\omega_1$ is the second harmonic frequency/frequency doubling frequency as shown in Figure 2.3

Figure 2.3: Second-harmonic Generation

2.3.2.1.4 Third Harmonic Generation

Third Harmonic Generations is also known as optical frequency multiplier. An optical frequency multiplier is a nonlinear optical device, in which photon interact with a nonlinear material, and merge effectively to form new photons with greater energy, producing higher frequency and shorter wavelength. Direct third harmonic generation (THG), also called frequency tripling) exists, and can be used to discover the interface between material of different excitability. It is similar second harmonic generation and produced higher frequency and shorter wavelength than second harmonic generation. It is widely used in high power lasers and inertial confinement fusion experiments.

2.3.2.1.5 Optical Rectification

Nonlinear second order susceptibility is the primary cause of origin of nonlinear optical processes. In second order susceptibility there are two different cases presented

$$\chi_{kij}^{(2)}(0,\omega,-\omega) = \chi_{jki}^{(2)}(0,\omega,\omega) \qquad Eqn.\ (2.30)$$

It consists of one real part and one imaginary part. The real part of $\chi_{jki}^{(2)}(0,\omega,\omega)$ defines Pockels effect or linear electro-optics. When an optical beam and a dc (or low frequency ac) electric field interact with a second order material, there is change in refractive index observed proportional to applied dc electric field. This process is known as Pockel's effect or linear electro-optic effect. This was first observed by a German physicist Friedrich Pockel in 1906 [13, 14] .Where else the real part of $\chi_{kij}^{(2)}(0,\omega,-\omega)$ define another process known as optical rectification. When two electric fields interact with each other in nonlinear medium results in a static electric field then the process is called optical rectification [16].

2.3.2.2 Third order nonlinear processes

Third order nonlinear processes are based on the term $\varepsilon_0\ \chi^{(3)}\ E^3$ in the polarization expansion of the Eqn.(2.27). The most general third order process nonlinear process involves the interaction of four different frequency connected by $\omega_1 + \omega_2 + \omega_3 = \omega_4$. The ω_1, ω_2 and ω_3 are distinct frequencies for third order polarization in NLO materials and are given by the equation below:

$$E(t) = E_1(t)\ e^{-tw_1} + E_2(t)e^{-t\,w_2} + E_3(t)e^{-t\,w_3} + \text{c.c} \qquad \text{Eqn. (2.31)}$$

When some of these materials interact with an optical field and a slow time varying external field, the change in the indices is quadratically related to the external field applied. This effect is denoted as Kerr effect. This effect was first reported by a Scottish physicist John Kerr in 1875. [17]. Kerr effect can be observed when a laser beam propagates through a third order material. Kerr effect is the change in

the refractive index of a material in response to an applied electric field and is given by the equation below

$$\Delta n = k\lambda E^2 \qquad (2.32)$$

Where Δn = change in refractive index,

K = Kerr co-efficient,

f = wavelength of the laser beam and

E = magnitude of the slow time varying electric field.

Where n_2 is the nonlinear refractive index and I is the intensity of the laser source.

$$\Delta n = n_2 I \qquad (2.33)$$

The nonlinear refractive index is related to the third order susceptibility χ^3 as per the equation below.

$$n_2 = \frac{12\pi^2\chi^3}{c^2 n_o} \qquad (2.34)$$

Where $n_o$the weak field refractive index of the material and c is is the speed of light.

When a laser source whose transverse intensity propagates through a nonlinear material, a phase delay due to Kerr effect deforms the wave front causing it to either focus or defocus depending on the sign of the nonlinear refractive index n_2 [13]. If n_2 is negative the material behaves like a negative lens which diverges the beam and is called self-defocusing. When n_2 the material behaves like a positive lens, it converges the incident beam is known as self-focusing.

2.4 Nonlinear optical materials

The field of nonlinear optics has witnessed exponential growth after the advent of laser since 1960. Nonlinear materials interact with high intensity light to produce nonlinear effect. Based on the composition, these materials can be primarily

be categorized into two classes organic and inorganic [18]. Inorganic NLO materials such as lithium niobate ($LiNbO_3$) or potassium dihydrogen phosphate (KH_2PO_4) are known to exhibit second harmonic generation (SHG) effect [19]. As a result during the last 40 year these inorganic materials have been seen dominating the world of nonlinear optics. Where else as far as organic materials are concerned, during the 1990's, p-electron organic materials were identified as promising candidates for nonlinear optical applications. However, more recent studies of NLO materials have focused on the use of organic materials with π-electron conjugated systems [20]. Such materials offer the advantages of larger optical nonlinearity and faster optical response. Other driving forces behind the recent development of organic NLO's include higher bandwidth, lower driving voltage, more flexible device design, and potentially lower processing cost [21]. In this section we will discuss about nonlinear optical materials .This section is divided into two subsections namely second order materials and third order materials respectively.

2.4.1 Second order Optical Material

In early 1960s development and characterization of nonlinear material was done on some criteria. These criteria includes the material must be non-centrosymmetric, must have excellent optical quality and high refractive index, must easily available etc. The first reported nonlinearity was observed in quartz when Franklin and co-workers recorded a very weak second harmonic signal in quartz using Q-switched ruby laser source [22]. In 1962 two research teams individually showed that phase matching in ammonium-dihydrogen phosphate (ADP) can result in significantly stronger second harmonic signals [23,24]. Two years later Boyd and co-workers reported lithium meta-niobate ($LiNbO_3$) to be "An efficient phase matchable NLO material."[25]. Further inquiries in $LiNbO_3$ showed some advantages and

disadvantages, but the despite this shortcoming this material is perhaps the most popular inorganic NLO material. Later several investigators presented the application of organic nonlinear material in various fields i.e. photovoltaic, photonic devices etc.

However these researchers reported the potential of organic materials in photonic devices much attention was given to inorganic materials in 1960s [26, 27]. This trend changed when Kutz demonstrated a powder technique to evaluate the optical nonlinearities in powder samples of materials. The shift in focus on organic nonlinear materials was due to the several advantages they have over their inorganic counterparts. Since NLO effects are electronic in nature, exceptionally high switching speeds can be attained [28].

2.4.2 Third Order Optical Materials

A wide range of materials have been invested for third order nonlinearities since for these materials did not require symmetry condition. Different techniques such as third harmonic generation (THG), degenerate four-wave mixing (DFWM and self-focusing techniques were used to determine third order susceptibility. However due to variability of the nature of experimental conditions used in the optical processes, it was difficult to compare the results initially. However the ongoing research from several years has made it possible to develop materials that have high third order. One such developed third order material is nonconjugated conducting polymers. A particular discussion has been done on nonconjugated conducting polymers as third order materials.

2.4.2.1 Nonconjugated conducting polymers (NCP)

It was reported back in 1988 by M Thakur that conducting polymers are not limited to conjugated systems alone. It was reported that with an appropriate substituent a backbone having an isolated double-bond structure may become

conducting. Thus new set of polymers came into existence called as nonconjugated conducting polymer. The first reported NCPs by Thakur and co-workers were: 1,4-cis-1,4-polyisoprene, 1,4-trans-polyisoprene and poly(dimethyl butadiene) [29]. Subsequently, poly(β-pinene) [30], polyalloocimene, polynorbornene and styrene-butadiene-rubber (SBR), [31] were shown by Thakur's group to belong to the class of nonconjugated conductive polymers. It was seen that the conductivity of the polymers increased many orders of magnitude with doping of iodine.

Upon doping these nonconjugated polymers, positive charges/holes are created at the isolated double-bond sites. There is also a formation of I_3^- upon doping. The hole is loosely bound to I_3^-. In short iodine dopant interacts with the double bond of the polymer backbone causing the double bond to lose an electron. The transfer of charges occurs due to the movement of the positive carriers or holes that are created upon doping. The =C-H bending vibration band of the polymer significantly reduced upon doping since the double bonds transformed into radical cations upon doping and charge-transfer . Thus nonconjucated polymers when doped with iodine which is an electron acceptor become electrically conductive. Moreover these nonconjugated conductive polymers have been shown to have quantum dot characteristics because of the confinement of charges within subnanometer domains. Such confinement has led to significantly larger third order optical nonlinearities for these systems compared to known materials and structures. When one or more free electrons are confined within a space typically ranging from a few nanometers to microns, the system is called as a quantum dot. The number of confined electrons, which can be accurately manipulated, dictates the size and shape of the q-dot. The behavior of quantum dots is analogous to that of atoms. Just as there are energy levels in atoms, q-dots also possess energy levels which exist due to the confinement of the

electrons. This leads to significant orders of magnitude enhancement of the third order optical susceptibility due to the confined electronic structure. A change in refractive index was reported in iodine doped1, 4-cispolyisoprene at 633nm for an applied voltage of 2V/μm. The corresponding Kerr coefficient was reported to be 1.6×10-10 m/V2 which is about 66.67 times higher than that of nitrobenzene measured at 589nm.[32] A modulation depth of 0.12% was reported in iodine poly(β-pinene) at 633nm.

2.5 FTIR Spectroscopy

FTIR stands for Fourier Transform Infrared Spectroscopy. FTIR is used mainly for characterization purpose. It can be used to indentify primarily chemicals that are organic and inorganic. It can also be used to analyze solids, liquids, gasses or to find a component in an unknown mixture. FTIR is perhaps the most powerful tool for identifying the functional groups or the type of chemical bonds in polymers. These functional groups include ketone, ester, acid etc. FTIR makes use of absorption, transmission and emission of light at different wavelengths to characterize any material. The wavelength of the light absorbed or transmitted is used to make structural characterization of the chemical bond in a polymer. By interpreting the infrared absorption, the chemical bonds in a polymer can be determined. FTIR spectra for of pure compounds are generally unique. As a result the spectrum of an unknown can be identified by comparison to the spectrum of known compounds. It gives peaks at different wavelengths depending on the vibrational energies of the chemical groups. Thus, each peak corresponds to specific chemical groups. Molecules consist of atoms with different bond lengths and bond angles. Moreover these bonds vibrate at different frequencies depending on the type of bonds. For any bond there is specific frequency at which it vibrates. Based on the different stretching and bending vibration

frequency corresponding different wavelengths or wave-numbers are determines , and groups like CH_2, CO, CH and NH groups can be identified [33]. The total transmission 'T' can be recorded as

$$T = \frac{I}{I_o} = e^{c\varepsilon l} \qquad Eqn.(2.35)$$

And the transmission can be converted into absorption by using the Beer Lambert Law.

$$A = -ln(T) = e^{c\varepsilon l} \qquad Eqn(2.36)$$

For example, chemical bond C-O absorbs near 1100-1300cm^{-1} and O-H group, absorbs strongly at ~ 3300-2500cm^{-1}. Ketone have strong absorption due to the presence of C=O carbonyl group near 1725-1705cm^{-1} [34, 35]. Similarly, the other organic functional group can be characterized.

2.6 Electro-Optic Effect

The electro-optics effect refers to the change in refractive index due to the applied electric field. If the change is linear to the applied electric field it is called linear electro optic effect. In this case the induced polarization of the material is linearly proportional to the electric field and is also termed as Pockels effect. Crystal having centered of symmetry show no linear electro-optics effect. There is induced index change that is directly proportional to the square of the electric field instead of varying linearly with it. In other words induced polarization in the material is quadratically proportional to the applied electric field. Such effect is also referred as Quadratic electro-optics effect or Kerr effect. This interaction of the optical radiation with the material subjected to an electric field can be described completely in terms of the impermeability tensor η_{ij} by the relation [36]

$$\vec{E}_i = \sum_j \eta_{ij} \vec{D}_j \qquad Eqn(2.37)$$

Quantum theory of solids, dictates that the optical impermeability tensor depends on the distribution of charges in the crystal. Application of electric field realigns these charges with a possible slight deformation of the ion lattice which causes change in the optical impermeability tensor. This change in the impermeability tensor can be related to the applied electric field by the following relation.

$$\Delta\eta_{ij} = r_{ijk}E_k + s_{ijk}E_k E_l \qquad Eqn.(2.38)$$

Where the r_{ijk} and s_{ijk} stands for linear electro-optic coefficient and quadratic electro-optic coefficient respectively. This quadratic electro-optics effect was first discovered by J. Kerr in 1875 in optically isotropic media such as glasses and liquids. Unlike linear electro-optic effect which is observed in anisotropic media, the quadratic electro-optic effect is seen in all media as there is no symmetry restriction. When an electric field is applied, the dimensions and orientation of the index ellipsoid change depending on the direction of the applied electric field and also on the symmetry properties of the 6 × 6 matrix elements of the s_{ijk} coefficient. The quadratic electro-optic coefficients for an crystal is given by

$$\begin{pmatrix} s_{11} & s_{12} & s_{12} & 0 & 0 & 0 \\ s_{12} & s_{11} & s_{12} & 0 & 0 & 0 \\ s_{12} & s_{12} & s_{11} & 0 & 0 & 0 \\ 0 & 0 & 0 & 1/2(s_{11}-s_{12}) & 0 & 0 \\ 0 & 0 & 0 & 0 & 1/2(s_{11}-s_{12}) & 0 \\ 0 & 0 & 0 & 0 & 0 & 1/2(s_{11}-s_{12}) \end{pmatrix} \qquad \textbf{Eqn (2.39)}$$

The index of ellipsoid for such an isotropic medium on the application of E reduces to

$$x^2\left(\frac{1}{n^2}+s_{12}E^2\right)+y^2\left(\frac{1}{n^2}+s_{12}E^2\right)+z^2\left(\frac{1}{n^2}+s_{11}E^2\right)=1 \quad Eqn.(2.40)$$

Where s_{12} and s_{11} are the quadratic electro-optic coefficients and E is the magnitude of the applied electric field.

$$n_0 = n-\frac{1}{2}\,n^3 s_{12}\,E^2 \qquad Eqn.(2.41)$$

$$n_e = n-\frac{1}{2}\,n^3 s_{11}\,E^2 \qquad Eqn.(2.42)$$

The birefringence $n_e - n_o$ is given by

$$n_e - n_o = n-\frac{1}{2}\,n^3(s_{12}-s_{11})E^2 \qquad Eqn\,(2.43)$$

By using the relationship $S_{44}=\frac{1}{2}(s_{12}-s_{11})$ can be written a

$$\Delta n = -n^3 s_{44}\,E^2 \qquad Eqn.(2.44)$$

Eq. 2.45 is often written in terms of the Kerr coefficient (K) in m/V^2 as

$$\Delta n = K\lambda\,E^2 \qquad Eqn.(2.45)$$

Where $S_{44}=-\frac{K\lambda}{n^3}$

This equation represents the relation between change in refractive index and the Kerr coefficient (K).

2.7 Differential Scanning Calorimetry (DSC)

DSC is used for thermal analysis of various materials. The different properties of the materials are been studied as they change with temperature. DSC curves reflect change in energy as function of time. In DSC two pans sit on an identical platform connected to a furnace by a common heat flow path and the entire working of the equipment is controlled by a computer. In one pan the polymers is placed and the

reference is in the other. The computer is programmed to increase the temperature of both the pans at same specified rate from one temperature to another. The computer makes sure that the heating rate stays exactly the same throughout the two separate pans in the experiment. The polymer is the one sample; it implies that it will take more heat to keep the temperature of sample pan increase at the same rates as the reference pan. The extra amount of heat required forms the basis of the DSC experiment. DSC graphs consist of temperature increase on the X axis and heat flow on the Y axis [37]. The whole plot finally will somewhat looks like this.

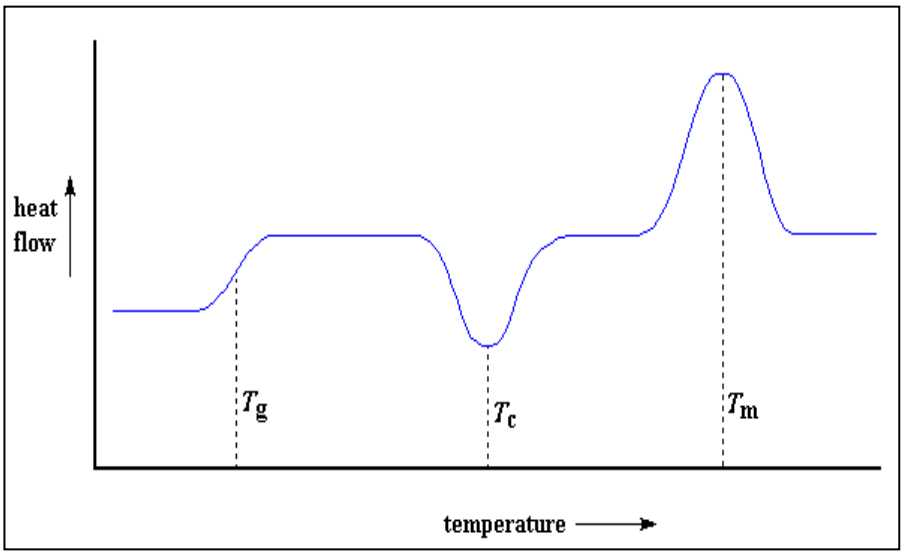

Figure 2.4: DSC plot of heat flow vs. temperature in a material

.

During the working the temperature of both the sample and reference are increased at a constant rate. Since the DSC is at constant pressure, heat flow is equivalent to enthalpy changes:

$$\left[\frac{dq}{dt}\right]_p = \frac{dH}{dt} \qquad \text{Eqn. (2.46)}$$

Here $\frac{dH}{dt}$ is the heat flow measured in mcal $sec^{-1.}$ The heat flow difference between the sample and the reference is

$$\frac{dH}{dt} = \left(\frac{dH}{dt}\right)_{sample} - \left(\frac{dH}{dt}\right)_{reference} \qquad Eqn.(2.47)$$

So in general differential scanning calorimeter is an instrument used for measuring specific heat capacities, heat flow rate, phase transition temperatures, glass transition (Tg) and melting temperature (Tm). Glass transition (Tg) is the phase change from amorphous solid into glassy liquid due to increase in temperature and also cause change in specific heat capacity [38, 39, 81]. Whereas melting temperature is that temperature at which, molecules of amorphous material get freedom to move, convert into crystalline phase. Thus DSC is an important tool in exploring thermal properties of materials.

2.8 Refractive index

In optics the refractive index of a medium is the measure of the speed of light in that medium. It is expressed as a ratio of the speed of light in vacuum to that in the considered medium [40, 41].

This can be written mathematically as:

$$n = \frac{c}{v} \qquad Eqn.(2.48)$$

Where c = speed of light in a vacuum.

v= speed of light in medium.

Refractive index is a function of frequency or wavelength. The relationship between relationship between relative permittivity 'ε' and relative permeability 'μ' is given in the Eqn. (2.49)

$$n^2 = \varepsilon\mu \qquad Eqn.(2.49)$$

$$\varepsilon = 1 + \chi \qquad Eqn.(2.50)$$

Usually at higher optical frequency, relative permeability of optical material become near unity.

This can be seen in the equation given below, which is obtained by substituting Eqn. (2.50) in Eqn. (2.49)

$$n = \sqrt{1 + \chi} \qquad Eqn.(2.51)$$

The refractive index for glasses and crystals are seen in the range of 1.4 – 2.8, lie in visible spectra region. Generally, semiconductors also show good nonlinear properties. A very good example is Gallium Arsenide (GaAs) with refractive index of ~3.5 at 1μm, due to strong absorption at different wavelengths below the band gap wavelength of ~870nm [42] It has also been seen that refractive index increase towards shorter wavelength; as can be seen for fused silica in Figure 2.5.

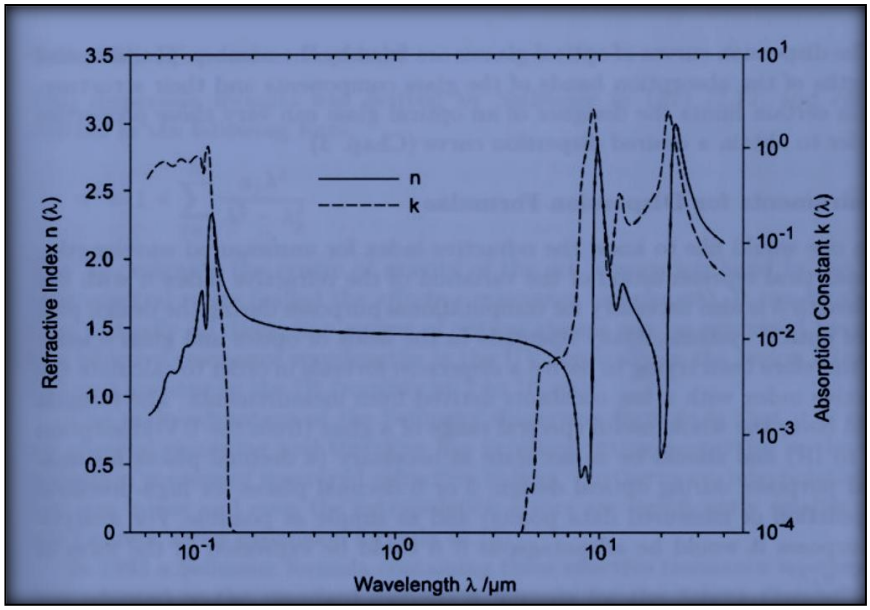

Figure 2.5: Refractive index and Absorption coefficient of fused silica (SiO_2 Glass) [46]

These nonlinear properties are expresses as complex number consisting of real and imaginary part similar to the refractive index, dielectric and susceptibility. The following equations given below represent the real and imaginary part relationship in susceptibility, dielectric and refractive index respectively.

$$\chi(\omega) = \chi'(\omega) + i\chi''(\omega) \qquad Eqn(2.52)$$

$$\varepsilon(\omega) = \varepsilon'(\omega) + i\varepsilon''(\omega) \qquad Eqn(2.53)$$

$$\eta(\omega) = n(\omega) + ik(\omega) = \sqrt{1 + \chi'(\omega) + i\chi''(\omega)} \qquad Eqn(2.54)$$

Where $n(\omega)$, $\chi'(\omega)$ and $\varepsilon'(\omega)$ and are real parts and $k(\omega)$, $\chi''(\omega)$ and $\varepsilon''(\omega)$ and are imaginary parts of refractive index, susceptibility and dielectric constant respectively.

2.8.1 Kramers- Kronig Relations in Nonlinear optics

Researchers Ralph Kronig and Hendrik Anthony Kramer together found a relationship between the real part and the imaginary part of the refractive index with the help of the theory on analytic complex numbers. [8, 44-46]. Similar relations between real and imaginary parts of the dielectric constant and susceptibility are given below in Eqn. (2.55) and Eqn. (2.56)

$$\varepsilon'(\omega) = 1 + \frac{2}{\pi}\int_{0}^{+\infty} \frac{\omega' \varepsilon''(\omega')}{\omega'^2 - \omega^2}\, d\omega' \qquad Eqn(2.55)$$

$$\chi'(\omega) = \frac{2}{\pi}\int_{0}^{+\infty} \frac{\omega' \chi''(\omega')}{\omega'^2 - \omega^2}\, d\omega' \qquad Eqn(2.56)$$

Refractive index expressed in term of absorption coefficient

$$n(\omega) = 1 + \frac{c}{\pi}\int_{0}^{+\infty} \frac{\alpha(\omega')}{\omega'^2 - \omega^2}\, d\omega' \qquad Eqn(2.57)$$

These Kramers–Kronig relations are very useful in nonlinear optics [47]. It relates the change in the refractive index caused by some excitation of a medium (e.g. generation of carriers in a semiconductor) to the change in the absorption (i.e. absorption coefficient). As the change in the absorption is normally significant only in a limited range of optical frequencies, it can be relatively easily measured. And the refractive index and reflectivity can be measured from the change in absorption coefficient respectively [8, 48].

Chapter 3

OBJECTIVES

The overall objective of this research is to explore the structural, photovoltaic and quadratic electro-optics effect of specific nonconjugated polymers. These polymers mainly include poly(β-pinene) (PBP), cis-1,4-polyisoprene (CPI) and trans-1,4-polyisoprene (TPI) and a copolymer styrene-butadiene-rubber (SBR)**.**

The structural changes in the molecular structure of a specific nonconjugated polymer SBR has been studied using FTIR, optical absorption, optical microscopy, before and after doping with iodine. The effect on specific heat capacity and the heat flow of specific nonconjugated polymers before and after doping were studied using a differential scanning calorimeter (DSC). The heat flow of these polymers has studies over a wide range of temperature from -50^0C to 110^0C. The effects on specific heat capacity of these nonconjugated polymers at specific temperature range before and after doping is also discussed. However further investigations have to be carried in this field.

The quadratic electro-optic effect in the styrene-butadiene-rubber co-polymer will be studied using field-induced birefringence technique, and the Kerr coefficients have be determined at 633nm and 1550 nm. The measured optical nonlinearities are been correlated to the nanometallic like structures of doped polymers.

The effect of using a doped nonconjugated polymer in a photovoltaic cell has been examined. The photovoltaic effect on the photocurrent due to the usage of nonconjugated polymer has been studied and discussed. Measurement and calculation of refractive indices of these novel nonconjugated polymers before and after doping are important. Linear absorption coefficients (UV-Visible) of styrene-butadiene-rubber have been measured for different doping levels of iodine. Refractive indices have been calculated using Kramer-Kronig transformation of absorption data for different doping levels. Numerical integration using MATLAB software was used for these calculations. Also the refractive indices of nonconjugated polymer, poly(β-pinene) (PBP) and SBR have been calculated at specific wavelengths 633nm by measuring reflectivity at 5^0, 10^0 and 15^0 angles of normal incidence respectively.

Overall this thesis will discuss the research study made on the structure properties, photovoltaic effect, electro-optics, refractive indices and thermal in specific doped nonconjugated conductive polymers and copolymer.

Chapter 4

NONCONJUGATED CONDUCTIVE POLYMERS

Organic polymers and inorganic materials have a wide range of applications in the field of photonics. Nonlinear optical properties of organic polymers have received substantial research attention in view of wide range of applications in the field of photonics especially in telecommunication photonics. Among organic materials, conjugated polymers having one-dimensional delocalization of electrons become electrically conductive upon doping. In 1988, M. Thakur demonstrated that with nonconjugated polymers with at least one double-bond in the repeat also become electrical conductive upon doping [31].

Recently, nonconjugated conductive polymers have been shown to have quantum dot characteristics because of the confinement of charges within subnanometer domains. Such confinement has led to significantly larger third order optical nonlinearities for these systems compared to known materials and structures. This has led to significant interest of researchers in the field of nonconjugated polymers. Since then various nonconjugated polymers have been researched by many researchers worldwide. This chapter illustrates literature review on specific non conjugated polymers that have been explored in this research work. These specific nonconjugated polymers include

poly(β-pinene) (PBP), cis-1,4-polyisoprene (CPI), trans-1,4-polyisoprene (TPI) and a copolymerstyrene-butadiene-rubber (SBR).Earlier study includes exploring the conductivity of non-conjugated polymers upon doping with iodine.Upon doping, there is formation of radical cation and charge transfer from double bond to dopant which is primarily responsible for the non-conjugated polymers to become conductive.It was found that the conductivity was based on the number of fraction of double bonds in the nonconjugated polymers. The ratio of double bonds to the total number of bonds along the polymer chain is termed as fraction of double bonds. Conjugated polymers have double bonds alternating with single bonds; as a result their number fraction of double bonds is 1/2, while non-conjugated conductive polymers have double bond number fractions less than ½. [29, 31, 32]. Mentioned below are few specific non conjugated polymers on which the research has been carried out in this work.

4.1 Poly (ß-pinene) (PBP)

PBP has been reported as novel nonconjugated polymer. It has ring type structure, with 1/6 number fraction of double since double repeat after every sixth carbon. The conductivity of PBP rapidly increases upon doping with iodine. The molecular structure of styrene –butadiene-rubber is shown in the figure below.

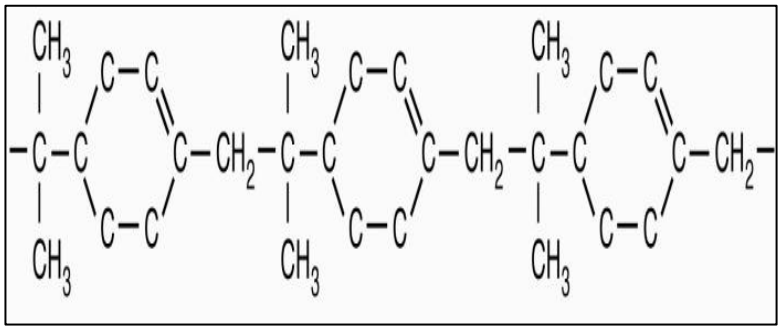

Figure 4.1: Molecular structure of poly(β-pinene)

Conductivity of PBP has been measured before and after doping with iodine, it increased by many orders of magnitude upon doping with iodine (0.008 S/cm). This is due to formation of radical cation and charge transfer from double bond to dopant. Earlier research show some characterization of PBP has been done by study of its thin film with optical absorption, FTIR, X-ray diffraction and other spectroscopic methods. PBP shows large nonlinear properties and have large Kerr coefficient, 1.6x10-10 m/V^2 at 1550 nm [49, 50]

4.2 Polyisoprene

Polyisoprene shows two conformations: trans-1,4-polyisoprene and cis-1,4-polyisoprene. These two conformations have same molecular formula but different orientation of carbon atom in the structure. Every fourth carbon atom in both the structure has double bond (number fraction of double bond is ¼). They have maximum conductivity of ~ 0.1 S/cm and the conductivity increases by many orders of magnitude after doping with iodine. [29, 32]

4.2.1 Trans-1,4-polyisoprene (TPI)

Trans-1,4-polyisoprene is a polycrystalline material with a planar zig-zag molecular structure. Recently it is known for its conductivity upon doping with iodine. The molecular structure of trans-1,4-polyisoprene is shown in the Figure below.

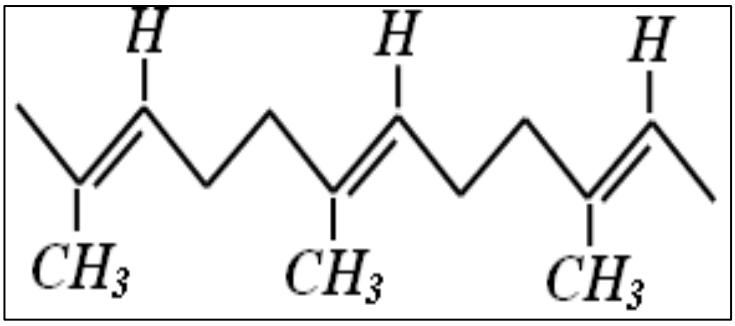

Figure 4.2: Molecular structure of Trans-1, 4- polyisoprene [51]

Characterization had done of TPI by study of its thin film with optical absorption, FTIR, X-ray diffraction. Kerr coefficient for trans-1,4-polyisoprene has already been reported to be 1.6x10-10 m/V2, which is higher than Poly(β-pinene) [29, 31, 51]. The above Figure shows a micrograph of trans-1,4- polyisoprene film.

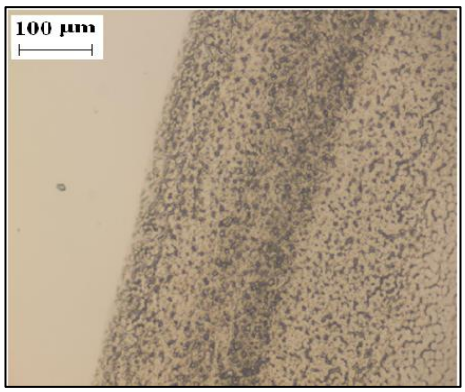

Figure 4.3: Micrograph of trans-1,4- polyisoprene film

4.2.2 Cis-1,4-polyisoprene (CPI)

Cis-1,4-polyisoprene is also known as natural rubber. It is a predominantly amorphous polymer and gives smooth film when deposited on glass slide from a solution. The electrical conductivity of cis-1,4-polyisoprene increases 100 billion times upon doping with iodine. The molecular structure of cis-1,4-polyisoprene is shown in Figure.4.4.

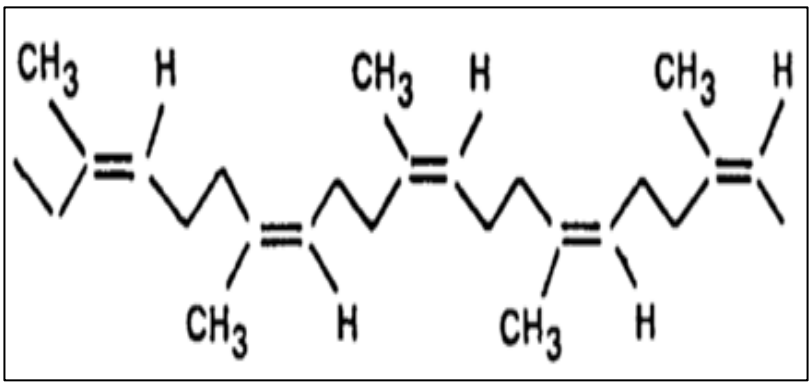

Figure 4.4: Molecular structure of Cis-1,4-polyisoprene.

The characterization of CPI of its thin film with optical absorption, FTIR, X-ray diffraction and other spectroscopic methods has been done earlier. Kerr coefficient for Cis-1,4-polyisoprene has been already reported to be 1.6x10-10 m/V2, which is higher than Poly(β-pinene) [29].

4.3 Styrene-butadiene-rubber (SBR)

Styrene-Butadiene-Rubber (SBR) is a synthetic rubber copolymer consisting of styrene and butadiene. It generally finds its application in car tires due to its ability to have good abrasion resistance [71]. Styrene-butadiene-rubber is nonconductive in its normal state. It becomes conductive upon doping with doping agents like iodine, SnCl4 and SbCl5. Styrene-butadiene-rubber was doped with iodine and it was noticed that the conductivity of the styrene-butadiene-rubber film reaches a value of about 0.01 S/cm and then the value remains a constant as the film is saturated with the iodine. The fact that the film darkens upon doping is attributed to the breaking up of the double bonds. The molecular structure of styrene-butadiene-rubber is shown in the Figure below.

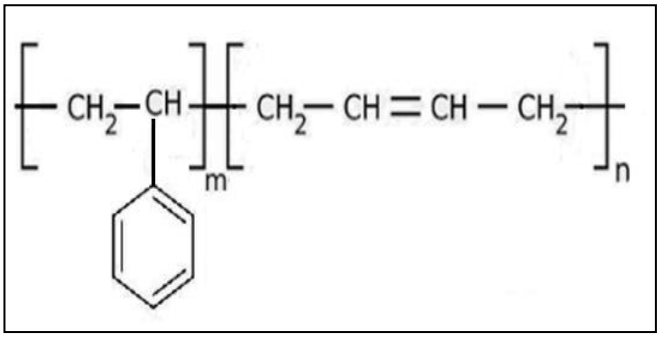

Figure 4.5: Molecular structure of styrene-butadiene-rubber.

Characterizations of styrene-butadiene-rubber using FTIR, optical absorption and DSC in this research work.

Chapter 5

COMPARISON OF OPTICAL PROPERTIES OF NANOMETALLIC AND DOPED NONCONJUGATED CONDUCTIVE POLYMERS

5.1 Introduction

Nano materials are the area of interest due to its wide application in the field of medical, military, biosensors, photovoltaic devices etc. The linear and nonlinear optical properties of the main reason for the wide range of application it has. They have a unique absorption, transmission and color spectrum pattern which depends on the shape, size and the surface of the nanoparticles.

When the nanoparticles interact with the incident light, electron and photons are excited at different wavelength and start oscillating. This results into unusual phenomenon known as Surface plasma resonances. This quality of nanoparticles decides the magnitude of strong absorption and scattering properties [52-54].This resonance is achieved at a specific wavelength and angle. It depends of the nanoparticle sample film, the frequency of plane polarized light and the refractive index of the media. Silver and gold nanoparticles are the most commonly known for surface plasma resonance. This was mainly because of the broad absorption band of wavelengths 400nm (near Ultraviolet) and 1000nm (near Infrared).

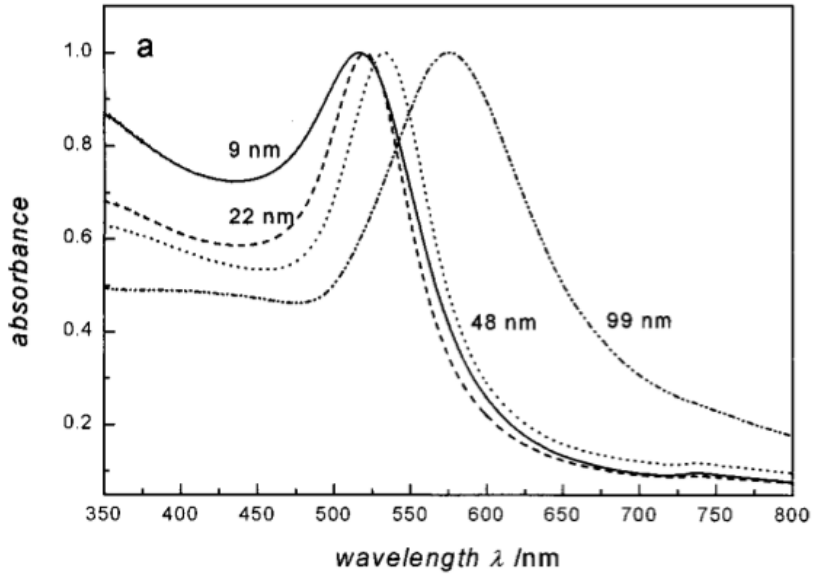

Figure 5.1 Absorption spectra of Gold nanoparticle of different diameter [55]

The above Figure clearly suggests that the absorption of gold nanoparticles surely depend on the size of the nanoparticles. As the size of the particle increases the absorption peak also increases. There is also a shift seen towards shorter wavelengths and broadness of peak becoming sharper as one goes from larger size to smaller size.

5.2 Nonlinear Optical Properties

Nonlinear optical properties of nanoparticles like Silver; gold and copper have been explored by many researchers. Higher optical absorption and large nonlinear properties have been seen in nanoparticles. Both these Third order susceptibilities and Kerr coefficient were measured by using Z-scan and it was reported that third order susceptility for nanometals is the function of frequency [57].At higher frequencies and shorter wavelength nanometals show larger kerr

coefficient and third order susceptibilty. Nonlinear absorption coefficient and susceptibility of copper nanoparticles in 2-Ethoxyethanol with 1 wt % PVP has been reported by *H. H. Huang et. al.* in 1997 [58]. They estimated third order absorption coefficient is about 15 $\times 10^{-10}$ m/W and $\chi 3$ is 4.27×10^{-11} esu. χ^3 for copper nanoparticles also reported by *A. Cetin et. al.*, about 1.55×10^{-10} esu [58]. *Hideyuki Inouye et. al* (1999) studied Kerr signal of Gold nanoparticles and estimates is about $\chi^3 = 2.0 \times 10^{-8}$ esu [59]. Nonlinear refraction and absorption coefficient at 532 nm laser of Au nanoparticles in water have studied by *J. T. Seo et.al*. He claims that the nonlinear absorption coefficient and refractive index were -1.89×10^{-9} m/W and 4.54×10^{-16} m^2/W respectively. The Figure given below shows the third order susceptibility in resonant region as shown in Figure 5.3 [60].

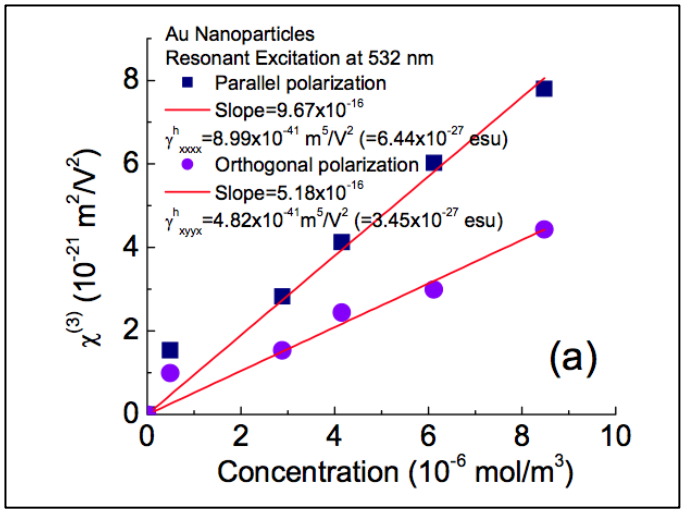

Figure 5.2: Third order susceptibility of gold nanoparticles with molar concentration

5.3 Comparison of Third order Optical Nonlinearities

Nonlinear properties of nanoparticles are applicable for ultrafast telecommunication, optical switching and other photonic devices. Recent research shows that both of the conjugated and nonconjugated polymers exhibit large nonlinear optical properties after doping with electron acceptors. Some of conjugated polymers,

i.e. PTS-polydiacetelene; nonconjugated polymers, i.e. cis-1,4-polyisoprene, trans-polyisoprene, they have given good response upon iodine doping. Kerr coefficient for cis-1,4-polyisoprene and trans-1,4-polyisoprene were found $1.6x10^{-10}$ (m/V^2) and $3.4\ x10^{-10}$ (m/V^2), which reflect that they are in nanometallic range. Table 5.1 comparing nonlinear properties of nanoparticles of metals and polymer.

Quantum Dots	**Wavelength (nm)**	**K (m/V^2)**	**$\chi^{(3)}$ (esu)**
Poly(β-pinene)	**1550 nm**	**$1.6x10^{-10}$**	**$3.4x10^{-8}$ Estd**
Cis-1,4-polyisoprene	**633 nm**	**$1.6x10^{-10}$**	**$3.4x10^{-8}$ Estd**
Trans-polyisoprene	**633nm**	***$3.4x10^{-10}$***	***$5.6x10^{-8}$ Estd.***
Poly(ethylenepyrrolediyl)	**633 nm**	**$1.2x10^{-9}$**	**10^{-7} Estd**
Cu : Al_2O_3	**575 nm**	**-----**	**10^{-8}**
Au : SiO_2	**532 nm**	**-----**	**$1.7x10^{-10}$**
PTS-polydiacetylene	**1550 nm**	**$3x10^{-12}$**	**$5x10^{-10}$**

Table 5.1: Third order nonlinear properties of nanoparticle and polymers.

Chapter 6

QUADRATIC ELECTRO- OPTIC EFFECT AND STRUCTURAL STUDIES OF NONCONJUGATED CO-POLYMER STYRENE-BUTADIENE-RUBBER

6.1 Introduction

Nonlinear optical properties of nano-optical materials have received significant research attention in the field of photonics application [1, 29, and 62]. In particular, third-order optical materials have attracted significant research interest due to their applications in various fields including electro-optic modulation, ultrafast switching, optical phase conjugation, optical limiting, etc. [2-4, 67]. Numerous classes of third-order materials have been investigated. Conjugated polymers such as polydiacetylenes were reported to have to high optical nonlinearities [3, 4]. These nonlinear optical properties are mainly attributed because of one-dimensional delocalization of electrons. Also recently, nonconjugated conductive polymers have been shown to have quantum dot characteristics because of the confinement of charges within subnanometer domains. Such confinement has led to significantly larger third order optical nonlinearities for these systems compared to knownmaterials and structures. Quadratic electro-optic effect in nonconjugated conductive polymers including cis-1,4-polyisoprene, 1,4-trans polyisoprene , poly(b-pinene), poly(ethylenepyrrolediyl) derivative and polynorbornene have been recently reported [36,50,69,70]. Exceptionally large Kerr-coefficients (about 30 times that of conjugated polymers) has been observed in these systems [36].

In this chapter, we discussed structural and nonlinear optical property; in particular, quadratic electro-optic effect in iodine doped styrene-butadiene-rubber film.

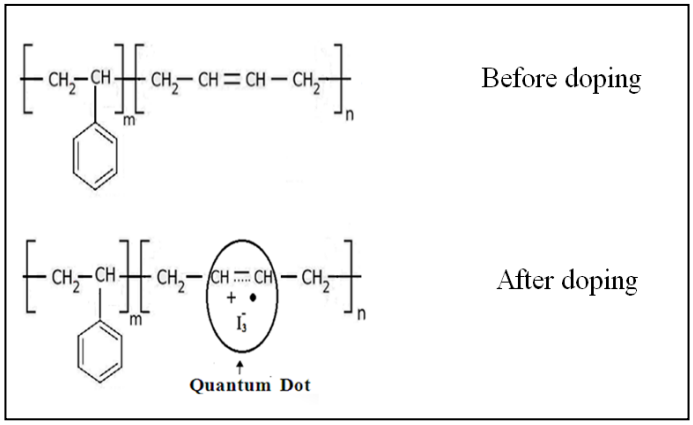

Figure 6.1: Transformation of double bond into cation radicals in SBR

Positive charge and cation radicals are confined near double in a sub nanometer domain as shown in Figure 6.1, which is less than a nano-scale. Below we have studied in detail the styrene-butadiene-rubber with the help of optical absorption, FTIR spectroscopy and its electro-optic effect has been measured.

6.2 Optical Absorption

Structural characterization of styrene-butadiene-rubber was conducted using optical absorption. Optical absorption measurements of the films were made using Ultrospec 2100 pro by Amersham Biosciences at various doping levels of iodine in styrene-butadiene-rubber. Sample made on glass slide were used for optical absorption. It was recorded that the absorption of undoped styrene-butadiene-rubber to be clearly transparent as shown in Figure 6.2.

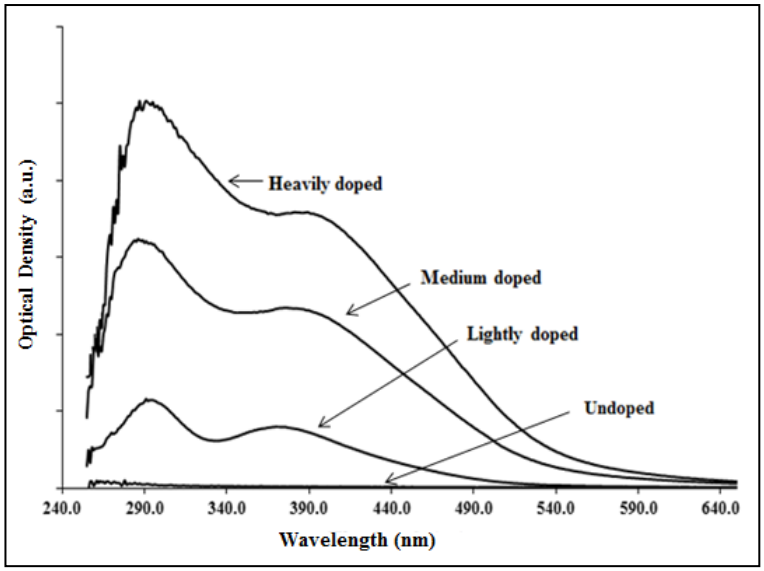

Figure 6.2: Optical absorption of styrene-butadiene-rubber

However upon doping it shows two peaks, one due formation of radical cations at 4.27eV and second due to charge transfer double bond to dopants (electron acceptors) at 3.2eV. It was also observed that upon increase in the concentration of iodine due to doping, peaks increases and peak correspond to 3.2eV widen ups and undergoes red shift due to reduction in separation distance between donor and acceptor. The optical absorption of silver nanocrystal has shown in Figure 6.3, indicate that absorption peak depends on size of nanoparticles; it increases with increase in size of particles [50]. Nonconjugated polymers have comparable optical absorption spectrum to the nanometallic absorption spectrum. The peaks of silver nanocrystal are at 425nm whereas the peaks of styrene-butadiene-rubber are less that 400 nm due to its charge confined in subnanometer domain which also suggests the nanometallic behavior or quantum dot characteristics of styrene-butadiene-rubber.

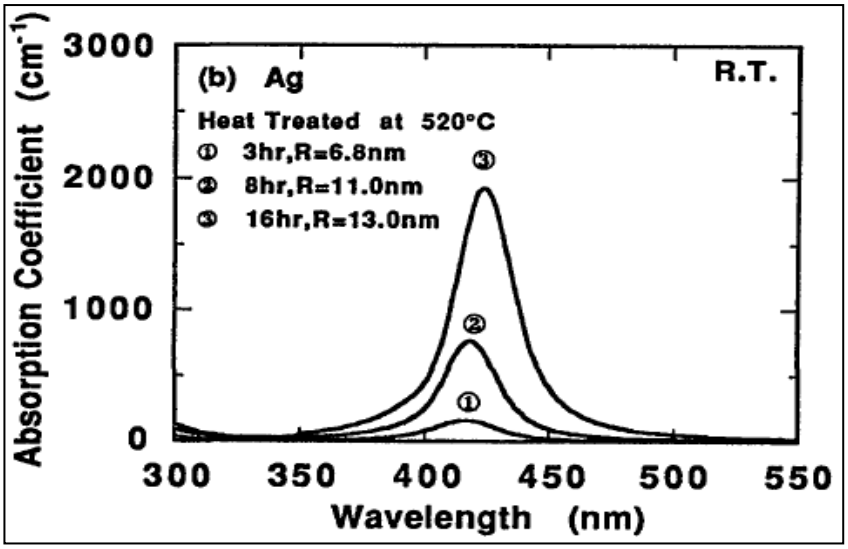

Figure 6.3: Optical Absorption of Silver Nanocrystal.

6.3 FTIR Measurements

The degree of conductivity of nonconjugated polymer depends on breakdown of double bond into radical cation and charges [73-75]. FTIR spectroscopy studies were done on styrene-butadiene-rubber both before and after doping with iodine. Thin samples were made of styrene-butadiene-rubber and FTIR spectroscopy was carried on them before and doping with iodine using Nicolet 6700 FTIR equipment. FTIR data indicated the =C-H vibration bands (964 cm^{-1} and 910 cm^{-1}) of polybutadiene decrease upon doping due to transformation of the double bonds into radical cation [72]

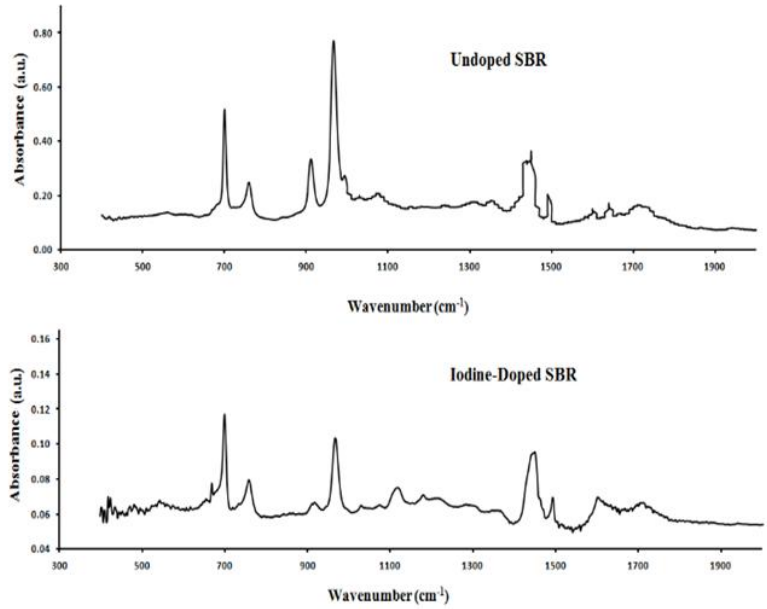

Figure 6.4 FTIR spectroscopy of SBR

6.4 Sample preparation for Electro-optics experiment

Sample of styrene-butadiene-rubber latex was obtained from the Goodrich Chemical company. As opposed to conjugated polymers, styrene-butadiene-rubber being a nonconjugated co-polymer is easily soluble in common organic solvents like toluene and chloroform. Thin films of SBR were prepared by dissolving SBR in chloroform on glass substrates. The rubber films thus obtained have a thickness of about 3.4 microns and 5 microns. The 5 microns thick sample was measured in 633 nm measurement, where else 3.4 microns was measured after 1550 nm measurement after the experiments have been performed. These films are held in a dish covered with aluminum foil and iodine equally placed besides it in the dish. Due to thermal evaporation of the iodine, the styrene-butadiene-rubber films get doped. On doping the films change color from colorless to black depending on the amount of dopant (i.e) iodine that has interacted with the styrene-butadiene-rubber film. The films were doped about 7 hours. The molecular structure of the undoped and doped

styrene-butadiene-rubber is shown in (Figure.6.1 and Figure.6.5) respectively. The doped sample is placed on copper electrodes with (optical glue) styrene applied between there surfaces. The sample is then mounted on a fixture to carry out electro-optics experiment.

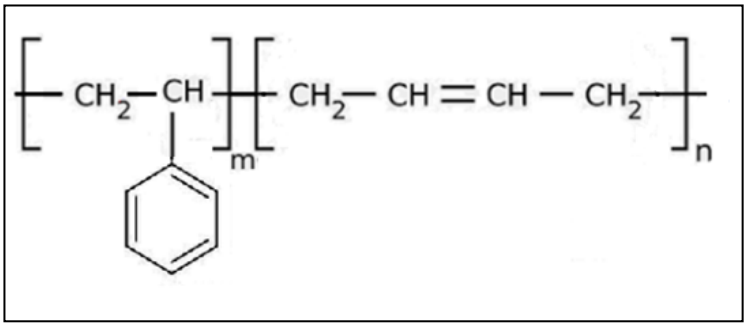

Figure 6.5: Molecular structure of undoped styrene-butadiene-rubber

6.5 Experimental setup

The high quality films on glass substrate were used to perform quadratic electro-optic measurements by field-induced birefringence technique at 633 nm and 1550 nm. A Helium Neon laser was used to make measurements at 633 nm and measurements at 1550 nm were performed using a semiconductor laser (BW-Tek). A schematic of the electro-optics set-up is shown in (Figure.6.6). The sample was placed between the polarizer and analyzer which were oriented orthogonal to each other to facilitate the polarization of the incident laser beam. This is also termed as Cross polarization.An AC voltage at 4 kHz was applied across the sample with the help of two copper electrodes to create an electric field. The modulation in optical intensity due to field-induced birefringence in the sample was measured using a photo-diode and a lock-in amplifier latched to twice the frequency of the applied field.

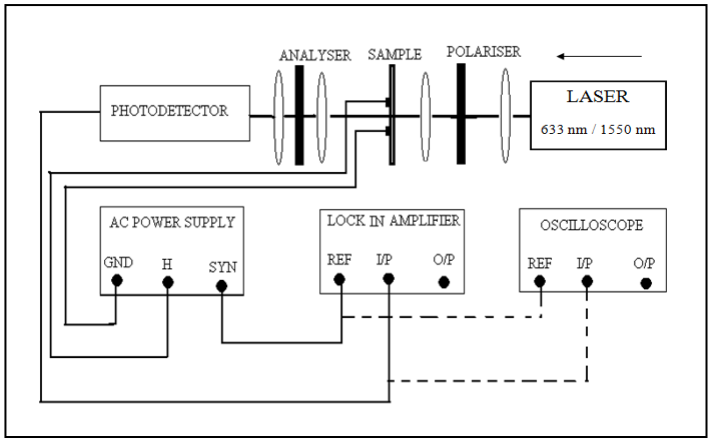

Figure 6.6: Experimental setup for electro-optics

6.6 Result and Discussion

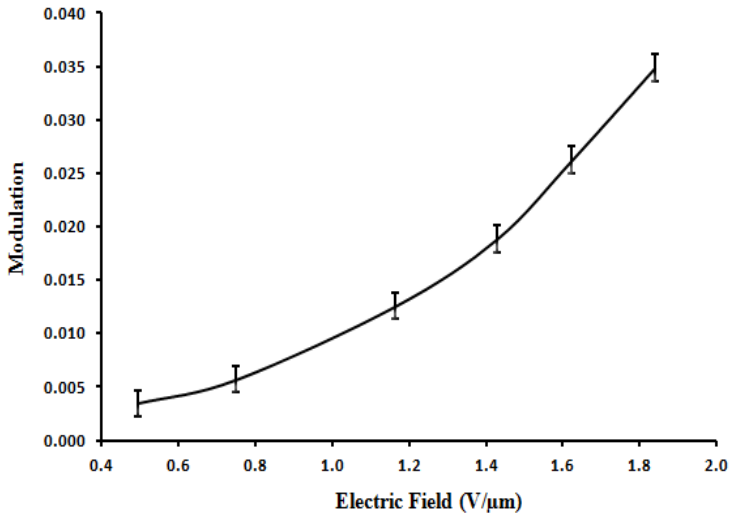

Figure 6.7: Quadratic modulation depth due to applied Electric field for 633nm

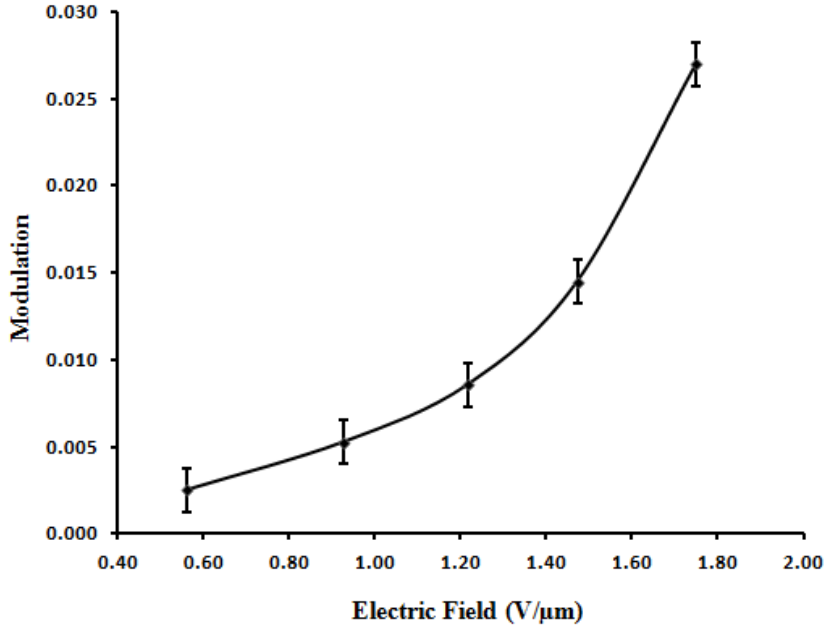

Figure 6.8: Quadratic modulation depth due to applied Electric field for 1550 nm

It was observed that the modulation depth quadratically varies with the applied field. A typical modulation depth vs. applied field plot is as shown in (Figure.6.7) and (Figure 6.8) for 633 nm and 1550 nm respectively. The Kerr coefficients as determined from these measurements are $3.1x10^{-10}$ m/V^2 at 633 nm and $1.2x10^{-10}$ m/V^2 at 1550 nm. The value at 633 nm is higher most likely because of resonant enhancement. These values are exceptionally large and slightly larger than that of doped cis-1,4-polyisoprene [16]. The value at 633 nm is about 129 times larger than that of the standard material nitrobenzene (Kerr coefficient is $2.4x10^{-12}$ m/V^2 at 589 nm). In comparison, the Kerr coefficient of PTS-polydiacetylene at 1.55 µm is $3x10^{-12}$ m/V^2 [17].

The large Kerr Coefficient is observed due to charge transfer involving double bond of nonconjugated polymer and the sub-nanometer size nanometallic domains (encircled Region in (Figure 6.1) formed upon doping. These structures particularly

represent novel metallic-like quantum dots of sub nanometer dimension for which enhanced optical nonlinearity can be expected. The electrical conductivity of these systems is comparable to that of metallic quantum dots / nanoparticles [76]. The optical absorption maxima are at higher energies / shorter wavelengths compared to metallic quantum dots of some of the smallest sizes known (~ 6 nm) [77]. The broader line-width of the optical absorption maximum is consistent with that of a nanometal with sub nanometer domain size [78]. These characteristics are all consistent with those of nanometallics with subnanometer-size domains.

Material	**Wavelength (nm)**	**$\chi^{(3)}$ (esu)**	**Kerr coefficient** ($m/V^{2)}$
PTS-polydiacetylene	1550	$5x10^{-10}$	$3x10^{-12}$
Poly β-pinene	633	$2.6x10^{-8}$Estd.	$1.2x10^{-10}$
Cis – polyisoprene	633	$3.4x10^{-8}$Estd.	$1.6x10^{-10}$
Trans-1,4-polyisoprene	633	$5.6x10^{-8}$Estd.	$3.5x10^{-10}$
Trans-1,4-polyisoprene	1550	$4.0x10^{-8}$Estd	$2.5x10^{-10}$
Ag-SiO_2	1064	$7.3x10^{-10}$ [42]	$3.4x10^{-12}$ Estd
Cu-$SrTiO_3$	770	$6.5x10^{-11}$ [44]	$3.0x10^{-13}$ Estd
styrene-butadiene-rubber (SBR)	***633***	$4.97x10^{-8}$ Estd	$3.1x10^{-10}$Estd.
styrene-butadiene-rubber (SBR)	***1550***	$2.16x10^{-8}$ Estd	$1.2x10^{-10}$Estd

Table 6.1: Comparison of third order nonlinearities

6.7 Conclusion

Thin films of styrene-butadiene-rubber before and after iodine-doping have been structurally characterized using optical absorption and FTIR spectroscopy. The optical absorption spectrum at low doping shows two peaks at 4.27 eV due to radical cation and the other at 3.2 eV due to charge-transfer respectively. Doping leads to a reduction of the intensity of =C-H bending vibration-band 964 cm^{-1} due to formation of radical cations upon charge-transfer. Quadratic electro-optics of styrene-butadiene-rubber has been attributed first time in the field of photonics. Quadratic electro-optic measurements of doped styrene-butadiene-rubber have shown exceptionally large Kerr coefficients: $3.1x10^{-10}$ m/V^2 at 633 nm and $1.2x10^{-10}m/V^2$ at 1550 nm. These large nonlinearities have been caused due to the sub-nanometer size metallic domains (quantum dots) formed upon doping and charge-transfer involving this nonconjugated conductive polymer. These exceptionally large nonlinearities of iodine doped styrene-butadiene-rubber are important in ultrafast telecommunication devices and various other applications in photonics.

Chapter 7

STUDIES OF THERMAL PROPERTIES IN NONCONJUGATED POLYMERS USING DIFFERENTIAL SCANNING CALORIMETRY (DSC)

7.1 Introduction

Study of thermal properties, heat flow, specific heat capacities and phase transition temperatures are important for various applications in thermodynamics and nanoparticle technology fields. Thermal properties of polymers and nanoparticles got attention of researchers since last few decades. Nonconjugated polymers such as poly(β-pinene), 1,4-trans-polyisoprene, styrene-butadiene-rubber and cis-1,4-polyisoprene have shown few nanometallic and crystalline characteristics. Thermal properties of nonconjugated polymers such as poly(β-pinene) and trans-1,4-polyisoprene, styrene-butadiene-rubber and cis-polyisoprene using DSC graphs have been explored in this chapter. Heat capacities of these polymers before and after doping and corresponding effect on T_g and T_m of the polymers before and after doping have also been discussed considering the molecular and nano structures of these materials before and after doping.

7.2 Specific heat of Nano particles

Study of thermal properties of nano sized particles has shown that they exhibit higher specific capacity than composite bulk materials (about 10 to 12 times)

[79]. J.Rupp group in 1987 reported that two nano-crystalline metal particles, Cu and Pd have higher compared with polycrystalline. Nano sized particle have greater atomic vibration at high temperature, which leads increase in specific heat capacity [80]. Also in the case of CuO, R. S. Prasher observed that the shape of the particles does matter for heat capacity. It is seen that cubic and thin particles have greater heat capacity. Thus particle size and density does play a role in the heat capacity. Softer nanocrystalline particles have greater atomic vibration than microscopic particles resulting into greater heat capacity.

7.3 Differential Scanning Calorimetry (DSC)

Differential Scanning Calorimetry (DSC) is the most widely used technique of all the thermal analysis method. There are two different types of DSC-methods, namely heat flux DSC and the power compensated. In this research work we have used heat flux based DSC apparatus. The DSC equipment consists of two empty aluminum pans placed in an isolated chamber so that the initial temperature of both the pans remains the same. The polymer whose thermal properties has to be studied is kept in one pan which serves as sample pan and the other serves as reference pan. In a heat flux DSC machine the material whose thermal properties have to be measured is placed in aluminum pan. There is also an empty pan which serves as a reference pan. The degrees to which, the rate at which and the end temperature range for the pans are defined by the computer controlled heating program. The output graphs of a DSC are called thermograms. Thermograms are the plots of the difference of heat delivered to the sample and to the reference as a function of the sample temperature. There are various kinds of thermograms obtained from DSC analysis which gives different kinds of information. Thus differential scanning calorimeter is a conventional instrument used for measuring specific heat capacities, heat flow rate and phase

transition temperatures, glass transition (T_g) and melting temperature (T_m). Increase in temperature leads into change in phase of amorphous solids into glassy liquid; refer as glass transition (T_g) and it also cause change in specific heat of materials [80,81]. At very high temperature, molecules of amorphous material get freedom to move, convert into crystalline phase and further increment in temperature cause melting denoted as melting temperature (T_m) [81]. Glass transition and melting temperatures can be seen in DSC Plot in Figure (7.1)

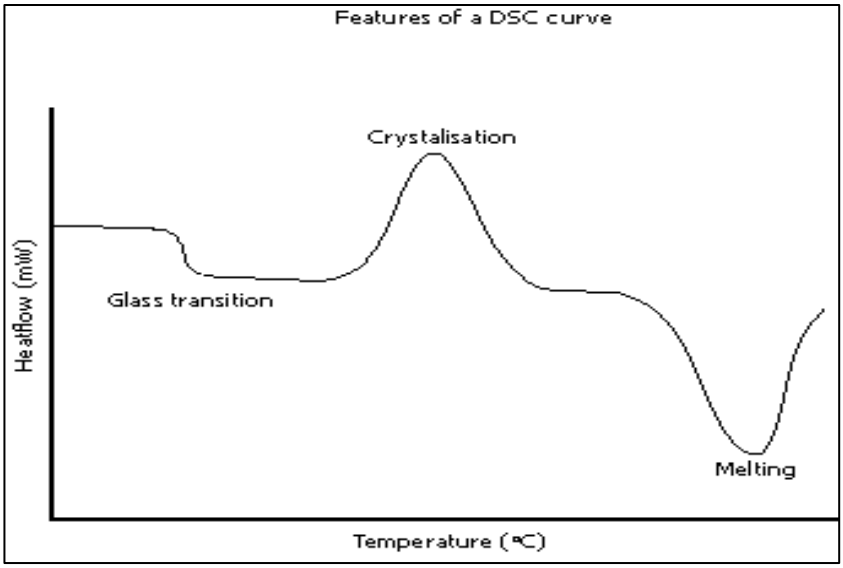

Figure 7.1: DSC plot of heat flow vs. temperature in a material

7.4 Experiments

Thin films of Poly(β-pinene), trans-1,4-polyisoprene were cast on quartz substrates from a toluene solution. But it was found that the film of trans-1,4-polyisoprene did not have good optical quality due to existence of microscopic or polycrystalline grains. This problem was overcome by adding a very small amount of C_{60} (~ 1% by weight of the polymer) to the solution. This procedure led to sharply reduced grain sizes and thus excellent optical quality films. Similarly Poly(β-pinene) crystals were dissolved in toluene solutions and were casted on quartz

substrate. The poly(β-pinene) films were doped with iodine for around 12 hours. These both doped and undoped high quality films then were finely powdered and were used in DSC. In the case of styrene-butadiene-rubber and cis-1,4-polyisoprene similar type of method was used. These rubbers were doped with iodine and powdered form was used in the DSC experiment.

7.5 Results

7.5.1 DSC of trans-1,4-polyisoprene.

Heat flow of doped and undoped trans-1,4-polyisoprene has been done on specific temperature range from -50^0C to 110^0C. The constant rate of increase in temperature was kept 5^0C. Graphs of rate of heat flow, specific heat capacity and temperature were obtained for trans-1,4-polyisoprene before and after doping with iodine.. The DSC results for trans-1,4-polyisoprene have been discussed first. Melting temperature peak of undoped trans-1,4-polyisoprene has been seen at 60^0C, which also reported by *Huafeng Shao et al* [40] for TPI with crystallinity about 50-60% and Edward G. *et al* also suggested that melting temperature (Tm) for low melting polymer about 64^0C [83,84].

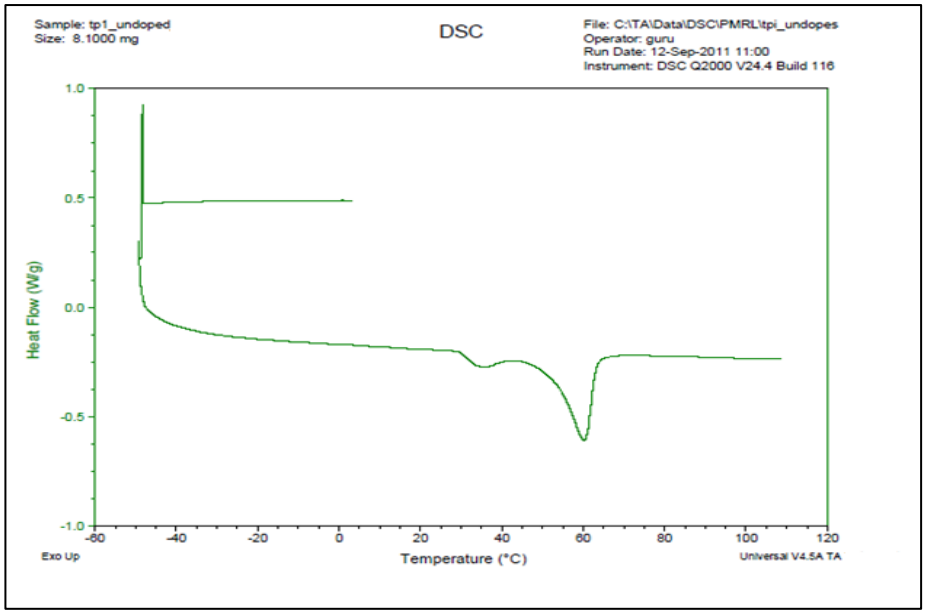

Figure 7.2: DSC scan of undoped Trans-polyisorene before doping.

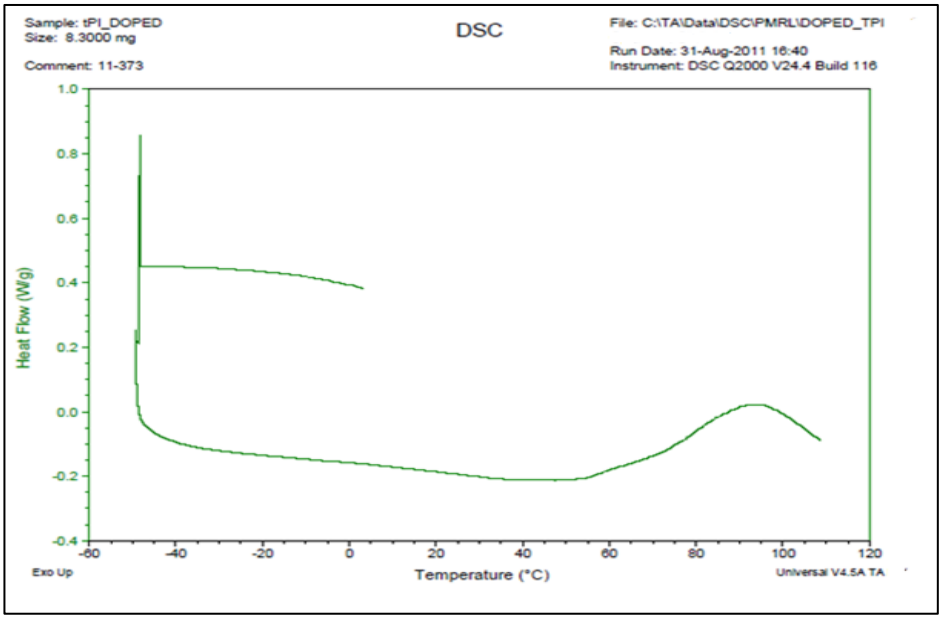

Figure 7.3: DSC scan of doped Trans-polyisoprene after doping

Melting peak can be seen clearly in Figure 7.1 at 60 ^{0}C, whereas after doping with iodine melting point was not well defined. Specific heat of trans-1,4-polyisoprene increased after doping with iodine. Figure 7.2 and Figure 7.3

shows heat capacity and heat flow of undoped and doped trans-1,4-polyisoprene for temperature range 10^0C -30 ^{0}C .

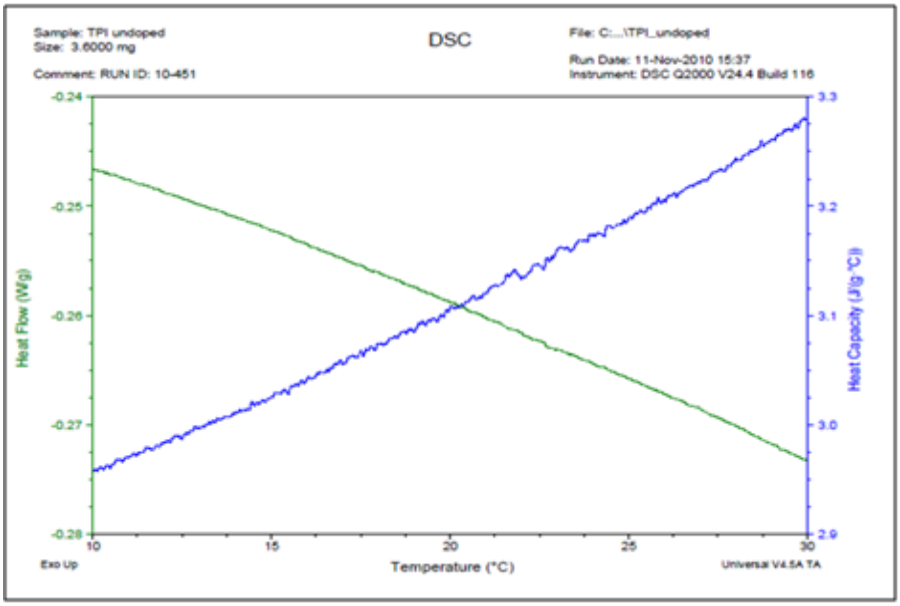

Figure 7.4: DSC scan of trans-1,4-polyisoprene before doping (0^0C to 30^0C).

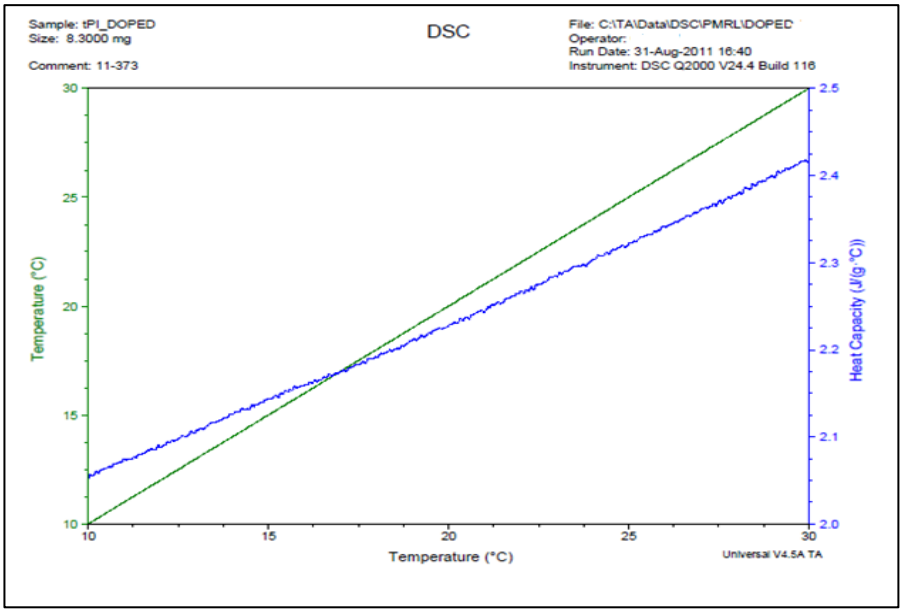

Figure 7.5: DSC scan of trans-1,4-polyisoprene after doping (0^0C to 30^0C).

It was observed in Figures 7.4 and 7.5 that specific heat capacities of trans-1,4-polyisoprene decrease around 30 degrees from 3.75 J/g^{0}C to 2.42 J/g^{0}C.

7.5.2 DSC of Poly(β-pinene)

DSC analysis for temperature range -50^{0}C to 100^{0}C was done for doped and undoped Poly(β-pinene) . It was observed that the melting temperature peak of undoped Poly(β-pinene) before doping has been seen at 77^{0}C . Whereas after doping it is not distinctly visible. It is found that the nature of the graphs obtained by the DSC of Poly(β-pinene) was in accordance to the graphs mentioned by An-Long Li, Xiao-Yan Wang, Hui Liang, Jiang Lu in 2006[85].

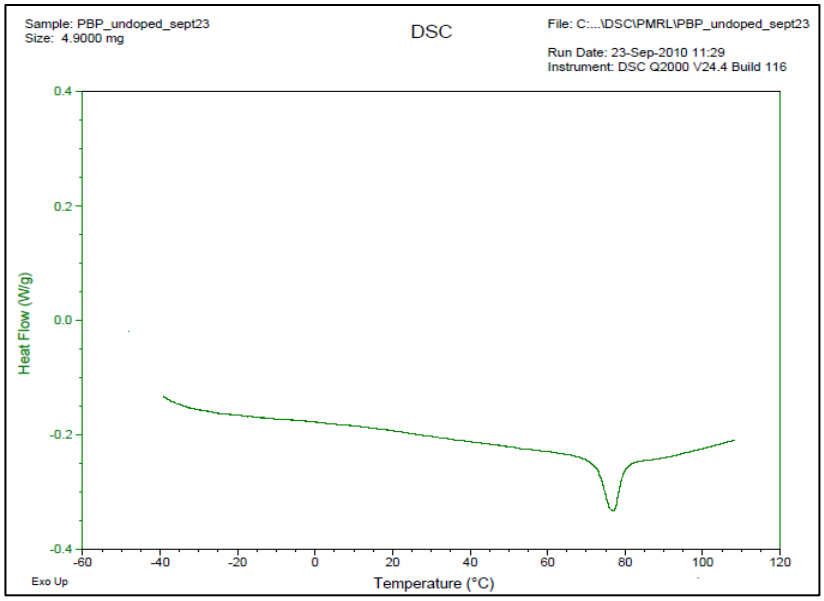

Figure 7.6: DSC scan of Poly(β-pinene) before doping.

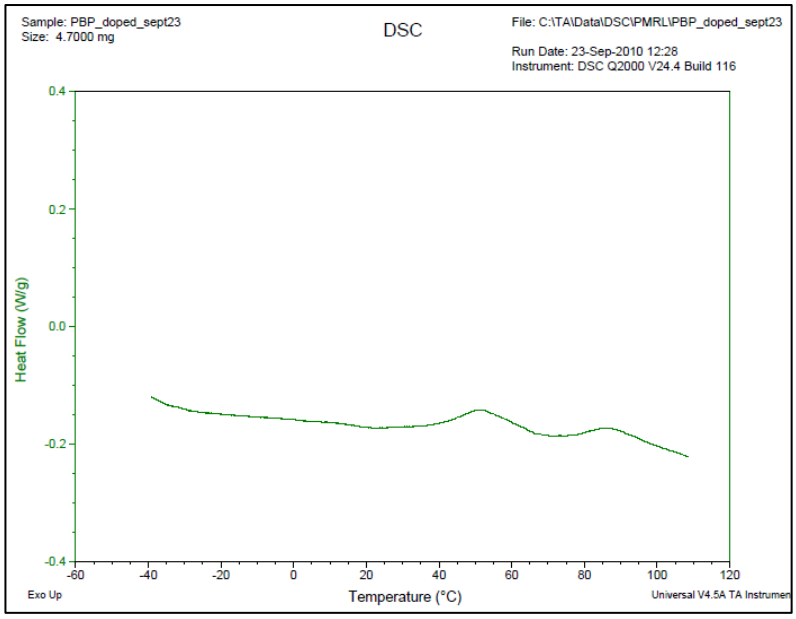

Figure 7.7: DSC scan of Poly(β-pinene) after doping.

Figures 7.6 and 7.7 shows heat flow of doped and undoped Poly(β-pinene) for temperature range -50^{0}C to 110^{0}C respectively. Specific heat of Poly(β-pinene) increased after doping with iodine. Glass transition for undoped Poly(β-pinene)appeared at 77^{0}C, but after doping the glass transition was not clear observed.

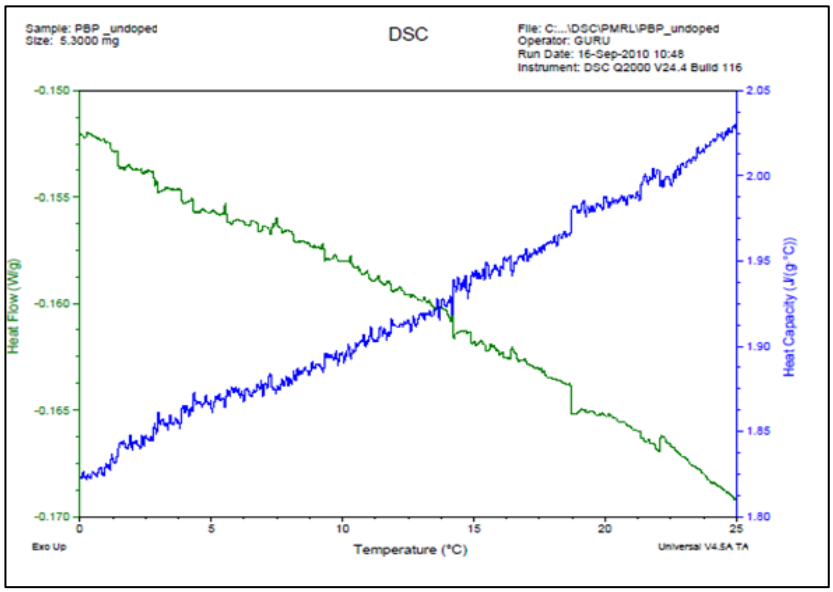

Figure 7.8: DSC scan of poly(β-pinene) before doping for the range (0^{0}C to 25^{0}C).

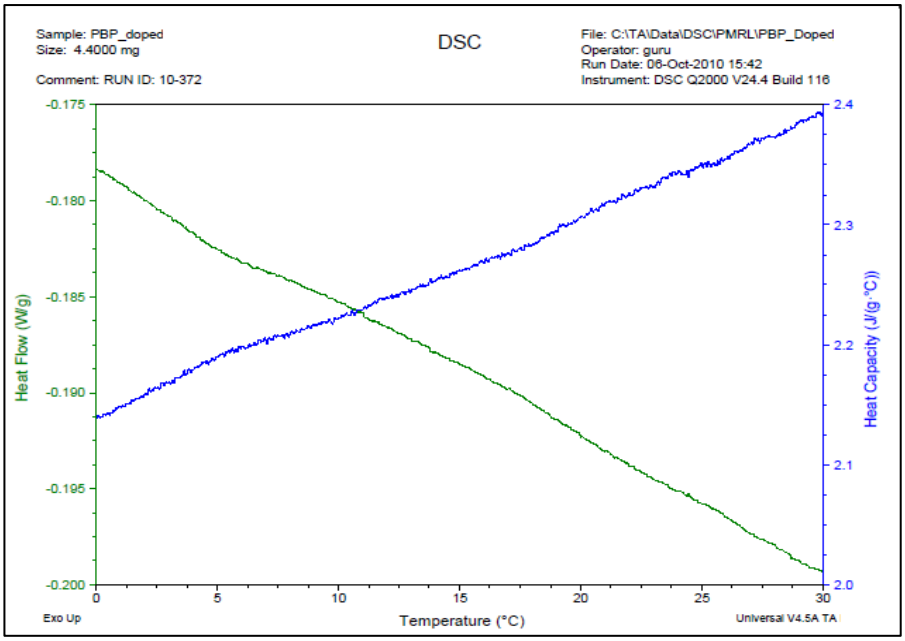

Figure 7.9: DSC scan of Poly(β-pinene) after doping for the range (0^0C to 25^0C).

The Figures 7.8 and 7.9 shows heat capacity and heat flow of doped and undoped Poly(β-pinene) for the temperature range 10-25^0C. It was observed in Figure 7.6 and Figure 7.7 the specific heat capacities of poly(β-pinene) increases around 30 degrees from 2.055 J/g^{0}C to 2.35 J/g^{0}C.

7.5.3 DSC of Styrene-Butadiene-Rubber

DSC analysis for temperature range -50^0C to 100^0C was done for doped and undoped styrene-butadiene-rubber. It was observed that the melting temperature peak of undoped styrene-butadiene-rubber before and after doping was not clearly observable. This can be attributed to the increase in rigidity upon doping which the polymer undergoes. It is seen that glass transition in SBR takes place at much lower temperature, and hence we cannot observe it in the graph below [61].

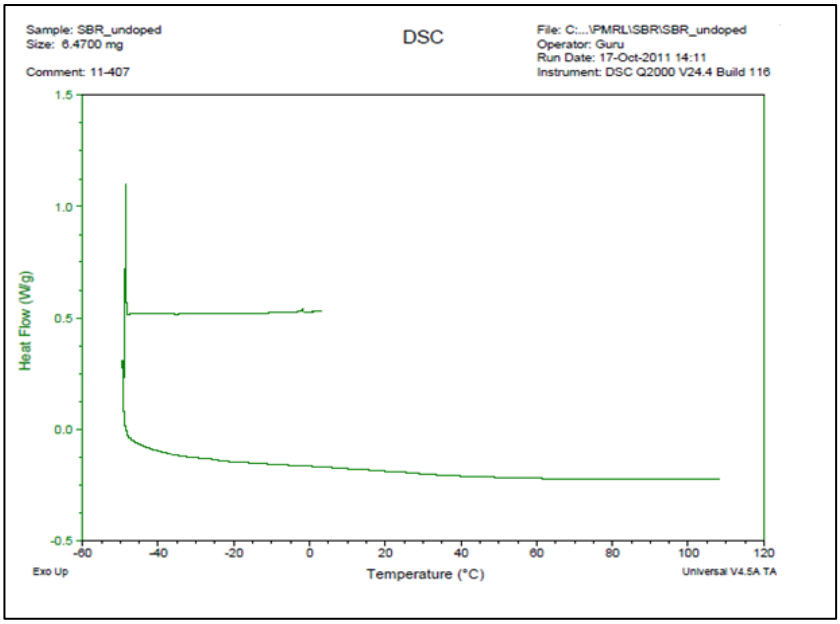

Figure 7.10: DSC scan of styrene-butadiene-rubber before doping.

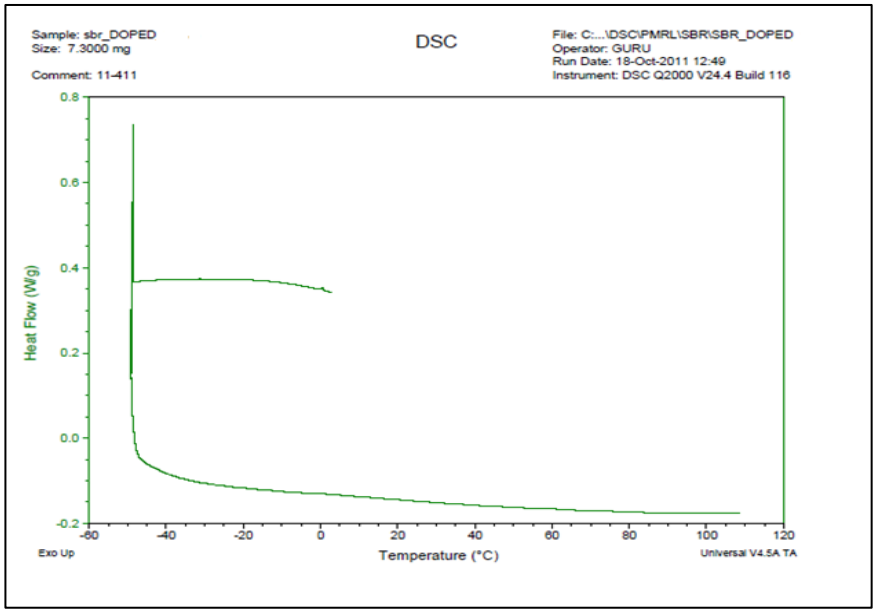

Figure 7.11: DSC scan of styrene-butadiene-rubber after doping.

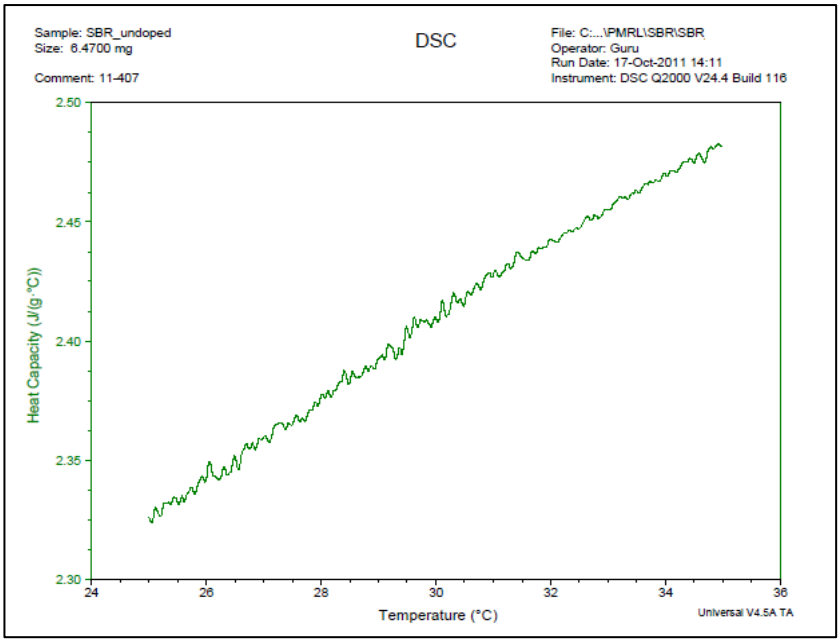

Figure 7.12: DSC scan of SBR before doping for the range (25^0C to 35^0C).

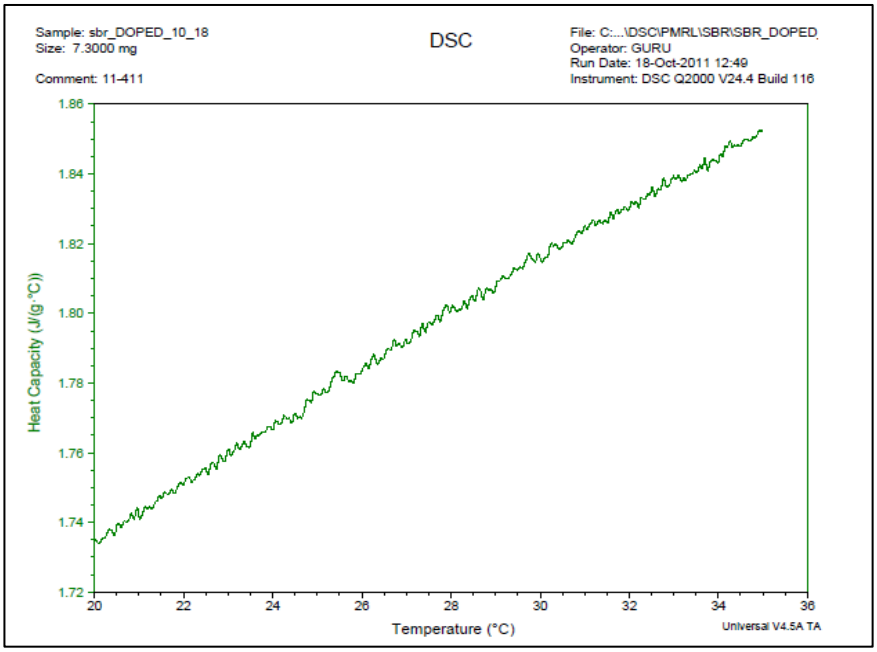

Figure 7.13: DSC scan of SBR after doping for the range (25^0C to 35^0C).

It was observed in Figures 7.12 and 7.13 that specific heat capacities of styrene-butadiene-rubber reduce around 30^0C from 2.425 J/g^{0}C to 1.86 J/g^{0}C.

7.5.4 DSC of Cis-1,4-polyisoprene

DSC analysis for temperature range -50^{0}C to 100^{0}C was done for doped and undopedcis-1,4-polyisoprene. It was also observed that the melting temperature peak of undoped cis-1,4-polyisoprene before and after doping was not clearly observable in the considered temperature range. It is observed that the glass transition of cis-1,4-polyisoprene takes place below the -50^0 C [66]. This can be attributed to the increase in rigidity upon doping which the polymer undergoes.

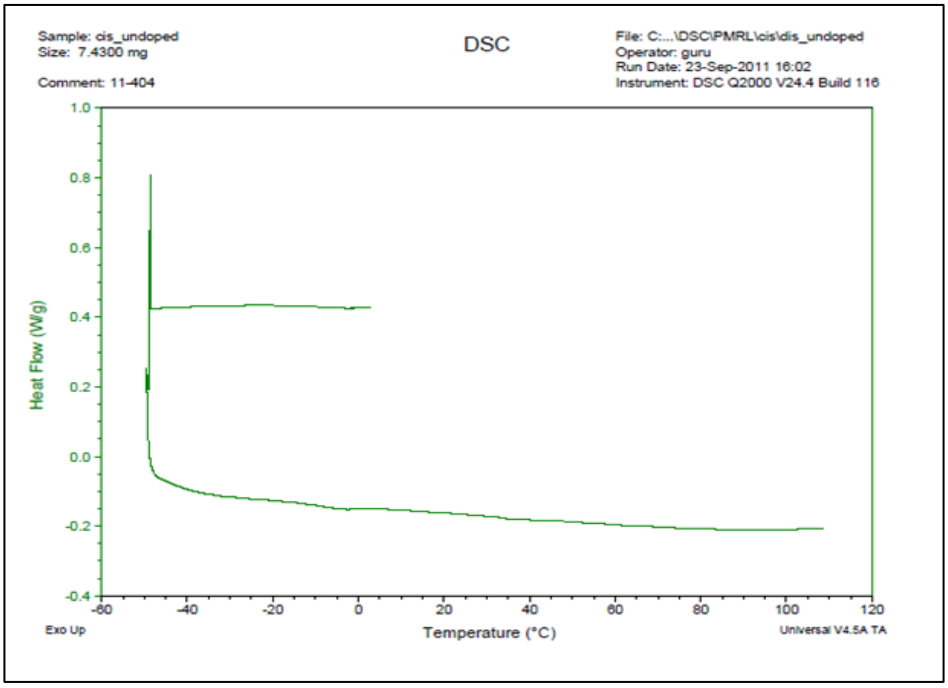

Figure 7.14: DSC scan of undoped cis-1,4-polyisoprene before doping.

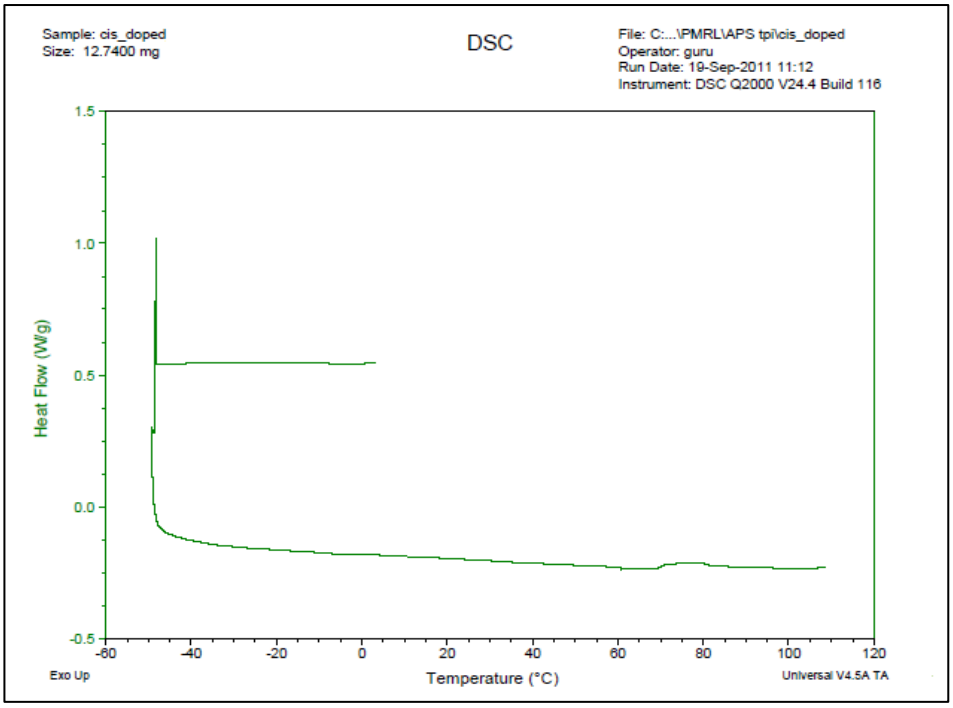

Figure 7.15: DSC scan of cis-1,4-polyisoprene after doping (20^0C to 35^0C).

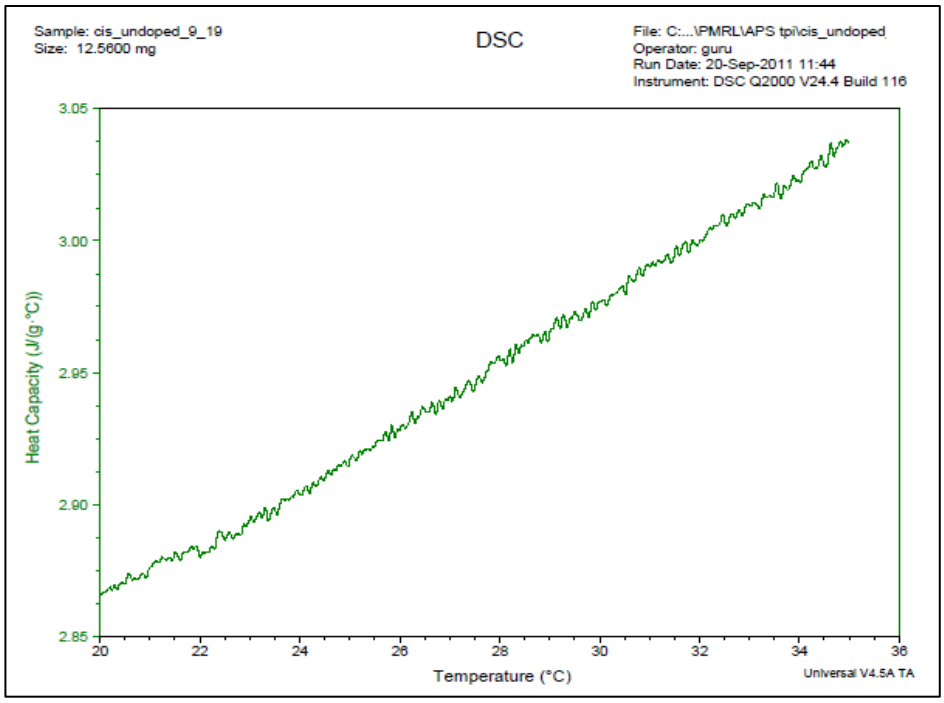

Figure 7.16: DSC scan of cis-1,4-polyisoprene before doping for the range (20^0C to 35^0C).

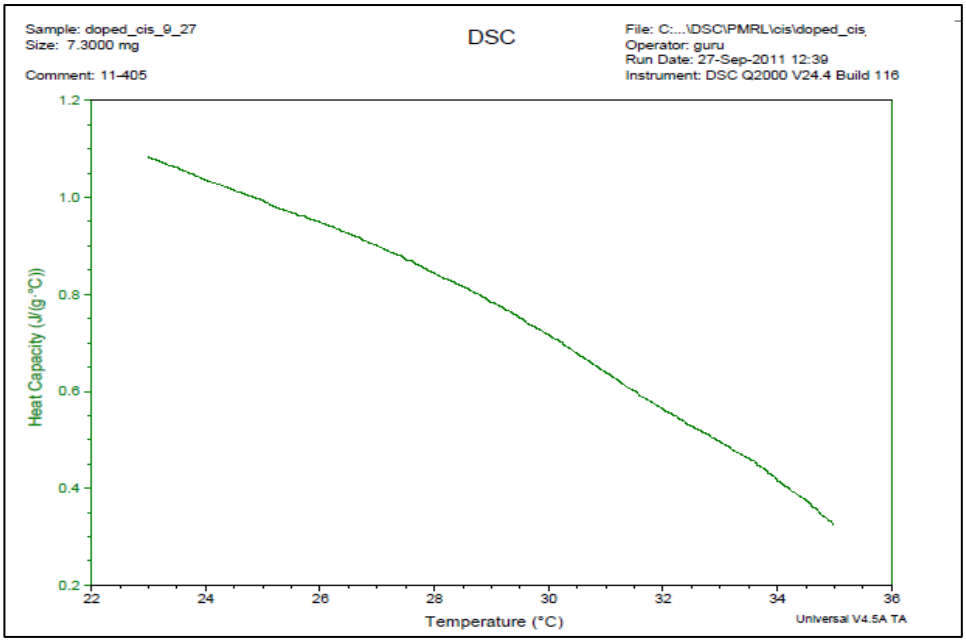

Figure 7.17: DSC scan of cis-1,4-polyisoprene after doping for the range (20^0C to 35^0C).

It was observed in Figure 7.16 and 7.17 that specific heat capacities of cis-1,4-polyisoprene reduce around 30^0C from 2.954 J/g^{0}C to 0.72 J/g^{0}C.

7.6 Discussion

It was observed that the specific heat capacity of poly(β-pinene) increases upon doping with iodine. However nonconjugated polymers like cis-1,4-polyisoprene, trans-1,4-polyisoprene and styrene-butadiene-rubber show decrease in the specific heat capacity upon doping with iodine. Upon doping, the double bond of these nonconjugated polymers transfers into cation radical and charge transfer takes place from double bond to the dopant. This confinement of charges within subnanometer domains gives rise to quantum dot characteristics (organic quantum dots). Such confinement gives significantly larger third order optical nonlinearities for these systems compared to known materials and structures. Studies have shown that these nonconjugated polymers upon doping show nanometallic type behavior due to the

formation of quantum dots [29, 31]. This phenomenon of nanometallic like behavior can bring out significant change in the specific heat capacity of the doped polymer as compared to undoped polymer. The earlier chapters illustrate the similar behavior of these quantum dots to the nano metals. The study of thermal properties of nano sized particles has shown that they exhibit higher specific capacity than composite bulk materials (about 10 to 12 times). In this case, such type of effect of increase in the specific heat capacity due to nanometallic like behavior of the polymer is found in poly(β-pinene) alone. While in the case of cis-1,4-polyisoprene, trans-1,4-polyisoprene and styrene-butadiene-rubber non metallic effect is dominated by iodine and elastomeric properties displayed by these rubber polymers. These polymers exhibit nanometal like behavior on doping with iodine. But since these polymers are elastic in nature (less rigid) the effect of this nanometallic behavior is superseded by iodine (Iodine has low specific heat capacity). Hence when iodine dominates the nanometallic behavior of these polymers, we can observe a decrease in the specific heat capacity upon doping. These polymers are more elastic unlike poly(β-pinene) which is glassy, hard and rigid at room temperature; this also influences the thermal properties of the polymer [61, 63-65]. The following table shows the change in specific heat capacities of specific nonconjugated conductive polymers before and after doping with iodine at 25^0C.

Nonconjugated Polymers	Undoped (J/g^{0}C.)	Doped (J/g^{0}C.)
PBP	**2.025**	**2.35**
TPI	**3.75**	**2.42**
CIS	**2.954**	**0.72**
SBR	**2.42**	**1.86**

Table 7.1 Specific heat capacities of specific NCP iodine doping at 25^{0}C.

7.7 Conclusion

Efforts were done to study the thermal properties of nonconjugated polymers including include poly(β-pinene) (PBP), cis-1,4-polyisoprene (CPI), trans-1,4-polyisoprene (TPI) and a copolymer styrene-butadiene-rubber (SBR) before and after doping. Thermal properties of the specific nonconjugated polymers before and after doping with iodine have been studied for a specific range (-55^{0}C to 110^{0}C). The effect on the heat flow for specific temperature range (-55^{0}C to 110^{0}C) and specific heat capacity were discussed. It was observed that specific heat capacity of poly(β-pinene) increases upon doping, while in the case of other nonconjugated polymer such as cis-1,4-polyisoprene, trans-1,4-polyisoprene and styrene-butadiene-rubber, the specific heat capacity reduces upon doping at 25^{0}C. The reduction in the specific heat capacity is found higher in cis-1,4-polyisoprene than trans-1,4-polyisoprene since the former is found out to be more elastic and its elasticity reduces more rapidly upon doping . The increase in the specific heat capacity of poly(β-pinene) which is glassy at room temperature was attributed to the formation of

organic quantum dots (similar to nanometallic quantum dots) upon doping. The T_m of undoped poly(β-pinene) and trans-1,4-polyisoprene has been found to be at 77^0C and 60^0C respectively. After doping the T_m transition was not clearly observable. In the case of styrene-butadiene-rubber and cis-1,4-polyisoprene, no significant transition in heat flow was found before and after doping with iodine. Thus line shape of the heat flow curves of styrene-butadiene-rubber a cis-1,4-polyisoprene do not change significantly upon doping with iodine for the specific rang (-55^0C to 110^0C). More detail studies need to be done in this field.

Chapter 8

PHOTOVOLTAIC EFFECT IN A COMPOSITE INVOLVING IODINE-DOPED POLY(β-PINENE), A NONCONJUGATED CONDUCTIVE POLYMER.

8.1 Introduction

Energy is a phenomenon which enables human beings to do work. All the day to day activities require some sort of energy to perform. In fact energy drives the universe. Sun is one of the most humongous sources of energy that we know till now. There are two types of energy source namely renewable and nonrenewable. The renewable consist of solar energy, wind energy etc where else nonrenewable consist of fossil fuels, oil, and petroleum etc.

However today, the need of exploring new ways to obtain energy from these renewable sources has gained attention of many researchers. This need is mainly due to the excessive utilization of nonrenewable resources in this modern world. The increase in world population is increasing the need for energy. It is estimated that the world population will be nearly doubled by the end of the twenty first century which will increase energy demand by nearly two times. The world population statistics from 1950 and the projected population statistics till 2050 are shown below [86].

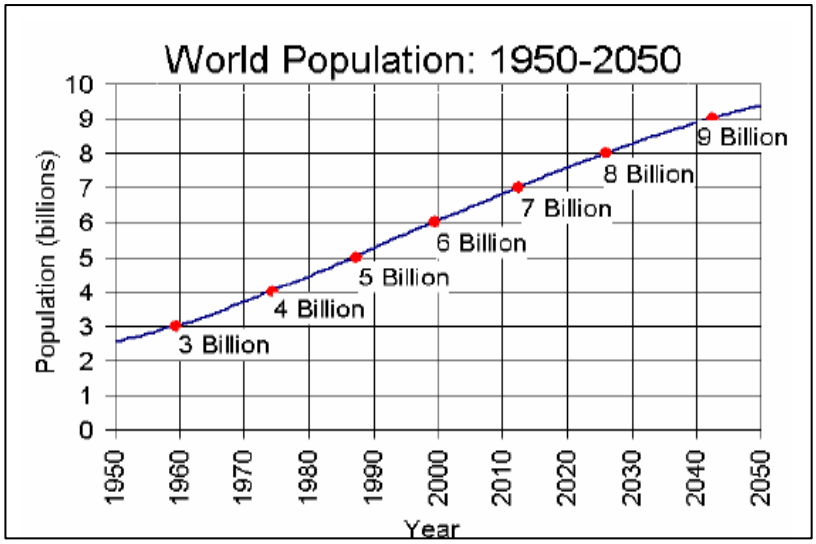

Figure 8.1 World Population statistics [86]

The population is projected to increase to 9 billion by 2042, which is nearly 50% increase from the year 1999 [86]. This would cause an increase in the world energy consumption. The world energy consumption from 1980 and the projected energy consumption till 2030 are shown below [87, 88].

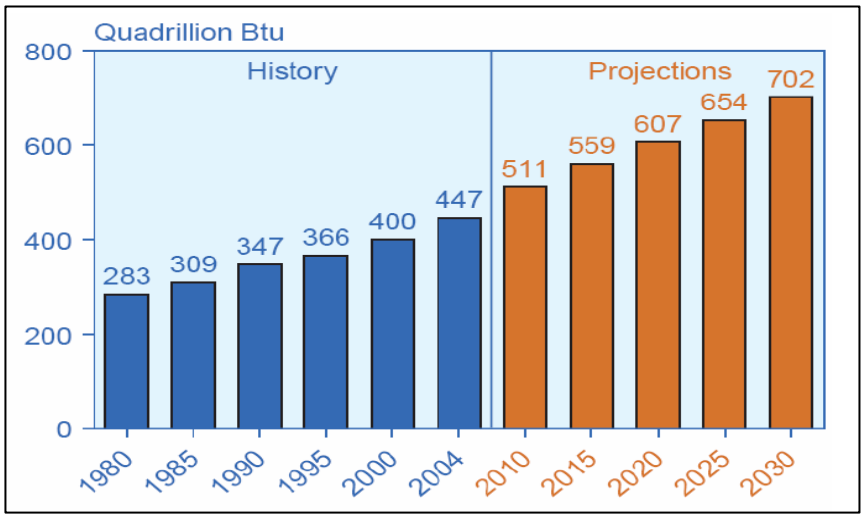

Figure 8.2 World Energy Consumption from 1980-2030 [87]

It is estimated that in 2030 the world energy need is projected to go nearly by 40%-50% of the present need. At present around 86.5% of the world energy needs are supplied through burning fossil fuels [89]. This has resulted into advent of the need

for exploring energy from the renewable resources. And photovoltaic is one such way to generate energy from a renewable source.

Organic polymers have attracted a great deal of interest in the area of photovoltaic. Photovoltaic are a field in which light energy is used to produce electric current by movement of free electrons. These materials show promising results and can serve as lower cost alternatives to inorganic photovoltaic materials [90]. The first two-layer organic photovoltaic system appears to have been reported in 1958 [91]. Poly (p-phenylene vinylene) (PPV) has been widely studied in the area of organic photovoltaic devices [92, 93, 94]. Exploration in the field of photovoltaic devices based on polythiopene has also been reported [91]. The incident light is responsible to produce electron from such organic materials resulting into generation of electric current. Earlier photo-induced electron-transfer between conjugated polymer and C_{60} leading to photovoltaic effects have been investigated in detail [95].

8.2 Experiment

Photovoltaic cells used in the report were formed by sandwiching the film of doped poly(β-pinene) between two electrodes. The carbon coated on the conducting side of tin oxide-coated glass slide was used as one electrode; where else the colloidal paste of the mixture of titanium-dioxide (T_iO_2), acetic acid and triton X-100 surfactant was coated on another conducting side of the other tin oxide coated glass slide. The film of the involving doped poly(β-pinene) was cast on the carbon electrode. The titanium-dioxide electrode was placed on a heater on a heat plate for about 20 minutes to get completely dry. Pressure by means of a clip was applied to keep the composite and the electrodes in contact. The film thickness was about 1 μm. Films thinner than that were not used in these experiments to avoid short-circuit between the electrodes. Carbon electrode was connected to the negative terminal of a high impedance electrometer (Keithley 617 Programmable

Electrometer) and the titanium-dioxide electrode was connected to the positive end of the electrometer to measure the photo voltage and photo current. The titanium-dioxide electrode was placed face-up to ensure that the light is incident on the polymer through this electrode. The experimental setup is shown in Figure. 8.3.

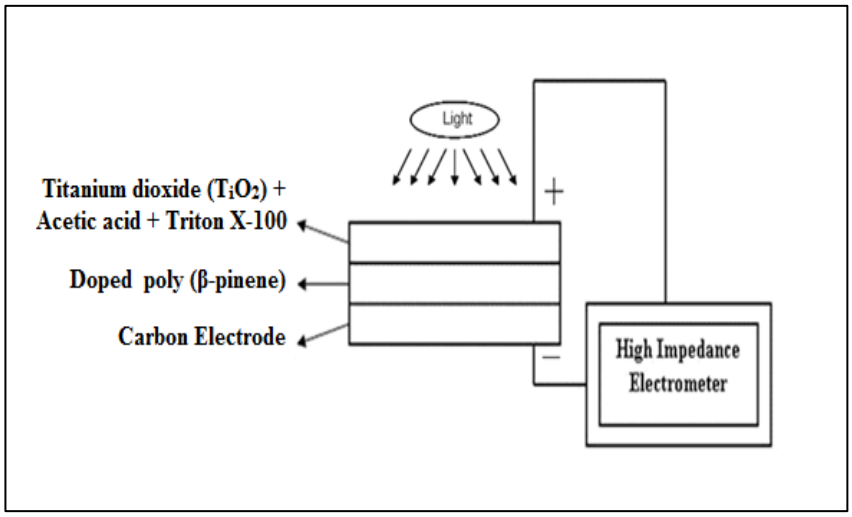

Figure 8.3: Experimental setup for photovoltaic

8.3 Results and Discussion:

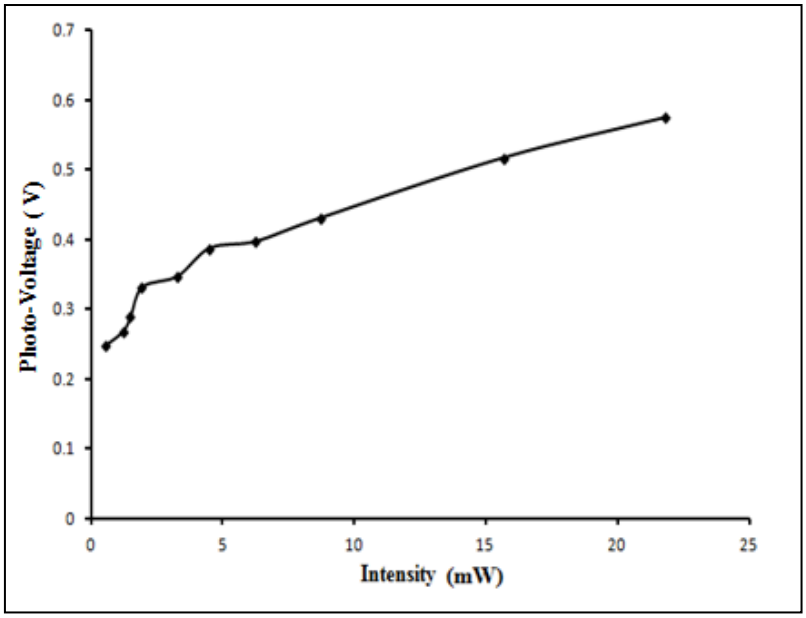

Figure 8.4: Plot of Intensity vs. Photo-Voltage

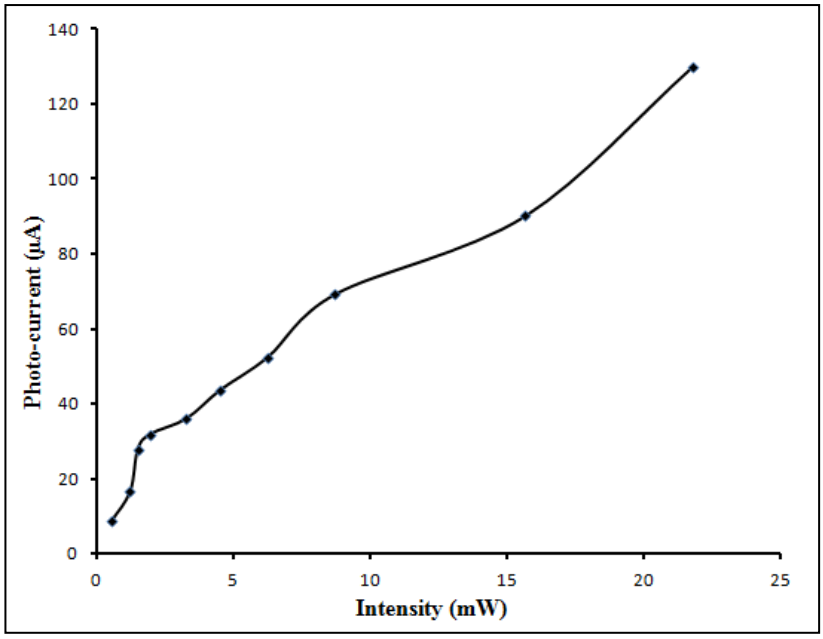

Figure 8.5: Plot of Intensity vs. Photo-Current

The graphs were plotted of Figure (8.4) intensity vs. voltage and Figure (8.5) intensity vs. current. It current and voltage was observed to increase as the distance of light source increases correspondingly. It is mainly because of the fact that the closer the light source the intensity of the light absorbs increases which increases the amount of released electrons. As the number of electron increase, the photo current increases. The photo voltage and photo current produced for a photovoltaic cell involving iodine-doped poly(β-pinene) was recorded to increase from 0.24V to 0.55V and 10µA- 130µA respectively. In this cell involving iodine doped poly(β-pinene) , the doped-nonconjugated polymer, iodine-doped poly(β-pinene) acts as an electron hole generator due to formation of radical cation and charge transfer between double bond to dopant upon doping. When the incident light is absorbed by the polymer, the electron hole pairs are produced which transfer the hole to the carbon electrode and electrons to iodine and ultimately to titanium dioxide electrode. This movement of electrons and holes are responsible for the observe photo voltage and photo current.

However further studies on efficiency and current ratings of the cells are under progress.

8.4 Conclusion:

Photo-induced charge transfer in an iodine doped poly(β-pinene) photovoltaic cell is observed for the first time. It is seen that as the intensity of the light increases the photo current and photo voltage increases. It is observed that the photo-voltage and photo-current increases from 0.24V to 0.55V and 10μA- 130μA respectively. This photovoltaic cell finds itself into various fields of applications providing cheaper cost in the areas of solar cells, photo-detectors, photo sensors etc.

Chapter 9

STUDY OF ABSORPTION COEFFICIENT AND REFRACTIVE INDICES OF NONCONJUGATED POLYMERS USING SPECIFIC METHODS

9.1 Introduction

In optics the refractive index in a medium is the measure of the speed of light in that medium [68]. Absorbance, also referred to optical density is due to the light absorption that occurs when atoms or molecules take up the energy of a photon of light, thereby reducing the transmission of light as it is passed through a sample. Attenuation of light takes place exponentially as it passes through the thickness of the sample and depends on the concentration of the absorbing species in the sample [70, 42].

Absorbance measurements are often carried out in analytical chemistry, since the absorbance of a sample is proportional to the thickness of the sample and the concentration of the absorbing species in the sample. Optical absorption coefficient data obtained from experimental measurements can be used to calculate refractive indices using a Kramers-Kronig relation which is discussed in the following.

9.2 Result and Discussion

The relationship between input-output intensities ratio and absorption coefficient is given by

$$\frac{I}{I'} = e^{-\alpha l} \qquad Eqn\ (9.1)$$

For the calculation convenience, the Absorption coefficient can be deduced from Eqn. (9.1) as follows

$$\alpha = \frac{\ln(I) - \ln(I')}{l} \qquad Eqn(9.2)$$

where I and *I'* are output and input intensities of light

'*l*' is distance travel by light, which is thickness of sample in this case

The above equation Eqn. (9.2) is used to calculate absorption coefficient from absorption data. Optical absorption of nonconjugated co-polymer styrene-butadiene-rubber has been studied at different doping level with iodine. As discussed earlier in chapter 6, the conductivity of styrene-butadiene-rubber increases by many orders of magnitude upon doping with iodine. The graphs obtain shows two peaks, one at 3.2 eV due to charge transfer from double bond to dopant or iodine, second at 4.27 eV due to formation of cation radicals. As the level of doping of iodine increases, the absorption peaks increases and as a result strong absorption is recorded. It is mainly because of more and more double bond transfer into cation radicals upon increase in the doping level, which cause strong absorption and higher absorption coefficient. The figure 9.1 shows, wavelength vs. optical density graph corresponding to heavily doped styrene-butadiene-rubber. Higher the doping stronger is the nanometallic characteristics in nonconjugated conductive co-polymer styrene-butadiene-rubber.

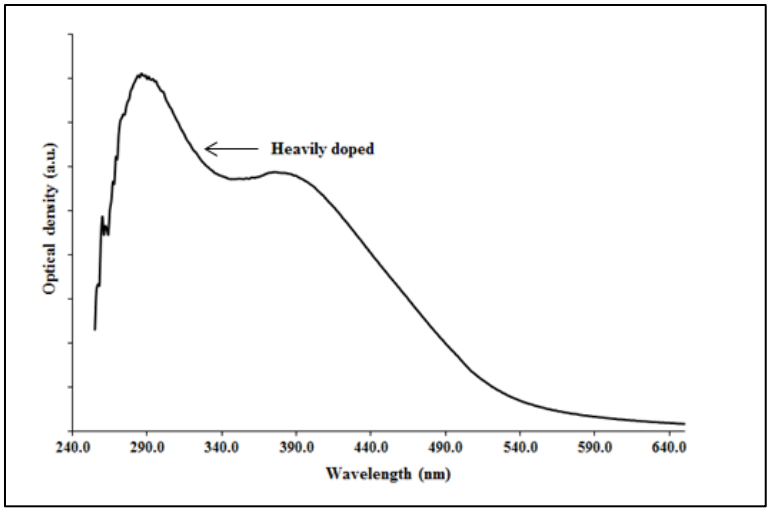

Figure 9.1: Absorption coefficient SBR at heavy doping with iodine

Similar absorption coefficient data was obtained for poly(β-pinene) at heavy doping with iodine. The further calculations were done using the expression that relates absorption coefficients to the refractive indices. Thus the refractive indices of iodine doped PBP have been calculated by numerical integration using Kramers-Kronig transformation, which is shown in Eqn. (9.2)

$$n(E) - 1 = \frac{ch}{2\pi^2} P \int_0^{\infty} \frac{\alpha(E')}{(E')^2 - (E)^2} \, dE' \qquad Eqn(9.3)$$

The Kramers-Kronig relation gives refractive indices as a function of energy. Numerical integration was done by using MATLAB software. The Figure 9.2 shows a plot of refractive indices in terms of their respective energies. Also it was observed that refractive index at 633 nm (2 eV) is 1.64.

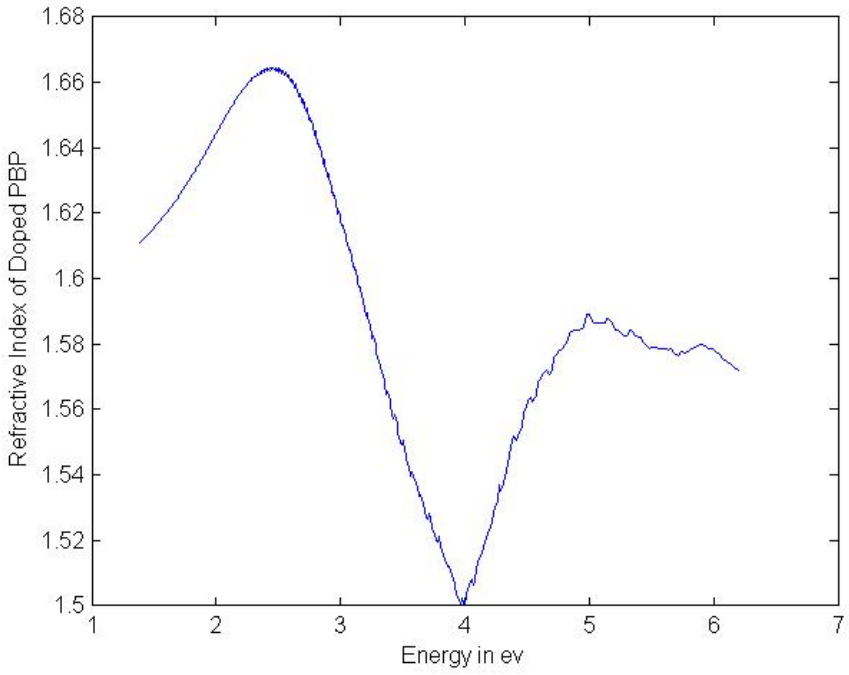

Figure 9.2: Refractive index of heavily doped PBP

Refractive indices at specific wavelengths 633 nm for heavily doped poly(β-pinene) and styrene-butadiene-rubber have been determined by measuring the incident and reflected laser light at different angles of incidence. The incident light was polarized parallel and in series to conduct the experiment. Polarized light waves are light waves in which the vibrations occur in a single plane. Experiments were carried out using thick samples of poly(β-pinene) and styrene-butadiene-rubber on glass slides and were heavily doped for a long time. Helium Neon laser was used to carry out the experiment. The incident laser beam light was polarized in parallel and in series by holding a polarizer in front of the laser. The intensity of the incident beam on the doped samples and corresponding intensity of the reflected beam from the doped sample were measured and refractive indices were calculated using MATLAB. The following formula was used

to find out refractive indices at various incident angles on the polymer for series and parallel polarization respectively.

$$r = \frac{n_1 \cos(i) - \frac{\mu_1}{\mu_2}^2 \sqrt{(n_2^2 - n_1^2 \ (\sin(i))^2)}}{n_1 \cos(i) + \frac{\mu_1}{\mu_2}^2 \sqrt{(n_2^2 - n_1^2 \ (\sin(i))^2)}} \qquad \text{Eqn 9.4}$$

Where $R = |r|^2$

The refractive indices for the iodine doped poly(β-pinene) were obtained for different angles with different polarization of the incident beams are as follows

Angle in degrees	**Refractive index in S-polarization**	**Refractive index in P-polarization**
5^0	**1.81**	**1.68**
10^0	**1.67**	**1.69**
15^0	**1.61**	**1.60**
	Avg = 1.69	**Avg =1.65**

Table 9.1 Refractive indices for different incident angles for PBP.

The refractive indices for the iodine doped styrene-butadiene-rubber were obtained for different angles with different polarization of the incident beams are as follows. These numbers for iodine-doped SBR may not be reliable because of the loss due to surface scattering.

Angle in degrees	Refractive index in S-polarization	Refractive index in P-polarization
5^0	1.33	1.30
10^0	1.32	1.31
15^0	1.32	1.32
	Avg = 1.32	Avg =1.31

Table 9.2 Refractive indices for different incident angles for SBR.

Refractive Index	By Kramers-Kronig Relation	By Reflectivity Experiment
Iodine doped PBP	**1.64**	**1.67**

Table 9.3 Refractive indices of iodine doped PBP at 633nm using specific methods.

9.3 Conclusion

Refractive indices of doped nonconjugated conductive co-polymers poly(β-pinene) has been calculated from absorption coefficients using Kramers-Kronig transformation upon high doping with iodine. Very large absorption coefficients and corresponding refractive indices have been observed for doped nonconjugated conductive co-polymers. Such large absorption coefficients are consistent with subnanometer metallic structure. These linear optical constants are vital to determine considering exceptionally large Kerr coefficients/third order susceptibilities of this nonconjugated

conductive co-polymer. The refractive indices for doped PBP and doped SBR were determined as (1.69 and 1.65) and (1.32 and 1.31) for S-polarization and P-polarization respectively. Also it was observed that the refractive index at 633 nm (2eV) obtained from Kramers-Kronig transformation of absorption coefficient are consistent with the measured values.

Chapter 10

SUMMARY

The research work performed in this project is summarized in the following. Structural studies of the nonconjugated co-polymer styrene-butadiene-rubber have been performed before and after doping with iodine. Quadratic electro-optics effect in styrene-butadiene-rubber after doping with iodine has been measured at specific wavelengths: 633nm and 1550nm.

The optical absorption spectrum of styrene-butadiene-rubber at low doping of iodine shows two peaks: one at 4.2eV due to radical cation and the other at 3.2eV due to charge-transfer. Doping leads to a reduction of the intensity of =C-H bending vibration-band ($964cm^{-1}$ and $910cm^{-1}$) due to formation of radical cations upon charge-transfer. Exceptionally large Kerr coefficients as measured $3.1x10^{-10}$ m/V^2 at 633nm and $1.2x10^{-10}$ m/V^2 at 1550nm are exceptionally large and have been attributed to the subnanometer size metallic domains (quantum dots) formed upon doping and charge-transfer.

Thermal properties of the specific nonconjugated polymers before and after doping with iodine have been studied for a specific range (-55^0C to 110^0C) using differential scanning caloriemeter. It was observed that specific heat capacity of poly(β-pinene) increases upon doping, while in the case of other nonconjugated polymer such as cis-1,4-polyisoprene, trans-1,4-polyisoprene and

styrene-butadiene-rubber, the specific heat capacity reduces upon doping. The difference has been attributed to the fact poly(β pinene) is glassy at room temperature while the others are partly or totally elastomeric. The T_m of undoped poly(β-pinene) and trans-1,4-polyisoprene has been found to be at 77^0C and 60^0C respectively. After doping the T_m transition was not clearly observable. In the case of SBR and cis-1,4-polyisoprene, no significant transition in heat flow line-shape was found before and after doping with iodine.

The reflectivity of iodine doped poly(β-pinene) and styrene-butadiene-rubber was calculated to be approximately 1.67 and 1.31 approximately. Also the refractive indices obtained from Kramer-Kronig transformation and 633 nm specific wavelength reflectivity experiments at approximately 633nm (2eV) were found to be approximately same (1.64 and 1.67). Photovoltaic effect in a composite involving nonconjugated conductive polymer; poly(β-pinene) (PBP) has been studied. Efforts were made to increase efficiency of photovoltaic cells by involving iodine doped specific nonconjuagted polymer poly(β-pinene) sandwiched between the two electrodes 1) Mixture of titanium dioxide, Triox-X and acetic acid and 2) carbon. However further research work has to be done in the field of refractive indices and photovoltaic involving doped specific nonconjugated polymers. Overall structural, optical, thermal, photovoltaic and quadratic electro-optic characteristics of specific nonconjugated conductive polymers including the co-polymer styrene-butadiene-rubber have been studied.

BIBLIOGRAPHY

1. M. Samoc, A. Samoc, B. Luther-Davis, Z. Bao, L. Yu, B. Hsieh, U. Scherf, J. Opt. Soc. Am. B 15 (1998) 817.
2. P.N. Prasad, D.J. Williams, Introduction to Nonlinear Optical Effects in Molecules and Polymers, John Wiley & Sons, Newyork, 1991.
3. R.W. Munn, C.N. Ironside, Principles and Applications of Nonlinear Optical Materials, Blackie Academic & Professional, USA, 1993.
4. J.M. Ballesteros, R. Serna, J. Solis, C.N. Afonso, A.K. Petford-Long, D.H. Osborne, R.F. Haglund Jr., Appl. Phys. Lett. 71 (1997) 2445.
5. M Born and E Wolf. Principles of optics: electromagnetic theory of propagation, interference and diffraction of light. Cambridge University Press, 1999.
6. D L Sengupta and T K Sarkar. Maxwell, Hertz, the Maxwellians and the early history of electromagnetic waves, volume 1. 2001.
7. G. P. Agrawal and R. W. Boyd,“Contemporary Nonlinear Optics”, Academic Press, 1992.
8. R. W. Boyd. Nonlinear Optics. Academic Press, 2003.

9. Y R Shen. The Principles of Nonlinear Optics. John Wiley and Sons, Newyork, 1984.
10. E G Sauter. Nonlinear optics. Wiley-Interscience, 1996.
11. A Yariv and P Yeh. Optical waves in crystals. Wiley New York, 1984.
12. N Bloembergen. Nonlinear optics. World Scientific, 1996.
13. R Paschotta. Encyclopedia of laser physics and technology. Vch Pub,2008.
14. H S Nalwa and S Miyata. Nonlinear optics of organic molecules and polymers. CRC press, 1997.
15. Mansoor Sheik-Bahae and Michael P. Hasselbeck, Department of Physics and Astronomy, University of New Mexico, Albuquerque, New Mexico "Third order non-linear properties"
16. Ananthakrishnan Narayanan "Electrical and Nonlinear Optical Studies of Specific Organic Molecular and Nonconjugated Conductive Polymeric Systems."
17. P Weinberger. Philosophical Magazine Letters, 8(12): 897–907, 2008
18. Alfa Aesar "Nonlinear Optical Materials"
19. L. R. Dalton, et.al., Chem. Mater., 1995, 7, 1060
20. (a) F. Pan, et.al., Appl. Phys. Lett., 1999, 74, 492; (b) T. Kaino, et.al., Adv. Funct. Mater. , 2002, 12, 599; (c) W. Geis, et.al., Appl. Phys. Lett., 2004, 84, 3729; (d) F. Pan, et.al. , Appl. Phys. Lett., 1996, 69, 13; (e) U. Meier, et.al., J. Appl. Phys., 1998, 83, 3486.
21. (a) L. R. Dalton, Pure Appl. Chem., 2004, 76, 1421.Y. Shi, et.al., Science, 2000, 288, 119; (b) L. R. Dalton, et.al., Adv. Mater., 2002, 14, 1339.

22. P A Franken; A E Hill; C W Peters; G Weinreich. Phys. Rev. Lett., 7: 118, 1961.

23. P D Marker; R W Terhune; M Nisenoff; C M Savage. Phys. Rev. Lett., 8: 21, 1962.

24. J A Giordmaine. Phys. Rev. Lett., 8: 19, 1962.

25. G D Boyd; C K N Patel. Appl. Phys. Lett., 5: 234, 1964.

26. P M Rentzepis; Y H Pao. Appl. Phys. Lett., 5: 156, 1964.

27. G H Heilmeir; N Ockman; R Braunstein; D A Kramer. Appl. Phys. Lett., 5: 229, 1964.

28. Ch Bosshard; K Sutter; P Pretre; J Hulliger; M Florsheimer; P Kaatz; P Gunter. Advances In Nonlinear Optics. Gordon and Breach Publishers, 1995.

29. M. Thakur, "A class of conducting polymers having nonconjugated backbones" *Macromolecules, 21* (3), pp 661–664, 1988.

30. H Rajagopalan; P Vippa; M Thakur. Appl. Phys. Lett., 88: 033109/1, 2006.

31. M. Thakur, "Nonconjugated conductive polymer" *J. Macromol. Sci., Pure Appl. Chem.*, A38 1337, 2001.

32. M. Thakur, R. Swamy. and J. Titus, "Quadratic Electrooptic Effect in a Nonconjugated Conductive Polymer" *Macromolecules, 37* (8), pp 2677–2678, 2004.

33. Found at internet address: http://www.wcaslab.com/tech/tbftir.htm

34. P. S. Kalsi, "Spectroscopy of Organic Compounds" New Age International, 2007

35. George Socrates, “Infrared and Raman characteristic group frequencies: tables and charts”, John Wiley and Sons, 2004.
36. Jitto Titus “Studies of the off-resonant nonlinear optical properties of an organic molecular crystal and specific nonconjugative polymers “.
37. PFEN 3100 (Polymer Engineering) at Auburn university “Fundamentals of polymer”.
38. SII Nanotechnology, “Specific Heat Capacity Measurement Using DSC-I” Japan (1981)
39. Bu-Xuan Wang, Le-Ping Zhou, Xiao-Feng Peng, “Surface and Size Effects on the Specific HeatCapacity of Nanoparticles” International Journal of Thermophysics, Vol. 27, No. 1, 139-151, (2006).
40. Hugh D. Young, Roger A. Freedman, University Physics, Addison-Wesley (2008).
41. Wolfram Research "Index of Refraction - from Eric Weisstein's World of Physics"
42. Found at internet address: Rudlger Paschotta , “Encyclopedia of Laser Physics and Technology” http://www.rp-photonics.com/refractive_index.html
43. V. Deiogio, Christos Flytzanis, “Nonlinear optical Materials: Principle and Applications”, Varenna on Lake Como, 1993.
44. D.C. Hutchings et al., “ Kramers-Kronig in nonlinear optics”, Opt. Quantum Electron. 24, 1, 1992.
45. Joseph Habib Simmons, Kelly S. Potter, “Optical materials” 2000.

46. V. Deiogio, Christos Flytzanis, “Nonlinear optical Materials: Principle and Applications”, Varenna on Lake Como, 1993.

47. D.V.G.L.N. Roa, P.Wu, B.R. Kimball, M. Nakashima, B.S. Decristofano, “Trends in Optics and Photonics”, 63, WB4/1- WB4/3, 2001.

48. Found at internet address: http://www.rp-photonics.com/encyclopedia.html.

49. P. Vippa, H. Rajagopalan, M. Thakur, “Electrical and Optical Properties of a Novel Nonconjugated Conductive Polymer, Poly(ß-pinene)”, *J Polym. Sci. Part B: Polym. Phys*. 43: 3695–3698, 2005.

50. A. Narayanan and M. Thakur, *Solid State Comm*., 150, 375, 2010.

51. S. Shrivastava, and M. Thakur “Quadratic electro-optic effect in the nonconjugated conductive polymer iodine-doped trans-polyisoprene, an organic nanometallic system”, Solid State Communication, 2011.

52. Li, W. R.; Xie, X. B.; Shi, Q. S.;, Zeng, H. Y.;, Ou-Yang, Y. S.; Chen, Y. B. *Appl Microbiol Biotechnol, 85(4),* 1115-22, 2010.

53. Lubick, N. Environ. *Sci. Technol*., *42 (23),* 8617, 2008.

54. S. L. Hsu, A. J. Signorelli, G. P. Pez, and R. H. Baughman, *J. Chem. Phys*., 69,1978 106.

55. Stephan Link and Mostafa A. El-Sayed, “Size and Temperature Dependence of the Plasmon Absorption of Colloidal Gold Nanoparticles” *J. Phys. Chem. B, 103,* 4212-4217, 1999.

56. Jirakorn ThisayuktaY, Hiroyuki Shiraki, Yoshio Sakai, Takenori Masumi, Sudarshan Kundu, Yukihide Shiraishi, Naoki Toshima and Shunsuke Kobayashi,“Dielectric Properties of Frequency Modulation Twisted Nematic

LCDs Doped with Silver Nanoparticles", *Japanese Journal of applied physics*, Vol. 43, 5430-5434, 2004.

57. R.H. Magruder III, Li Yang and R.F. Haglund Jr, "Optical properties of gold nanocluster composite formed by deep ion implantation in silica", *Appl. Phys. Lett.* 62(15), 1730-1732, 1993.
58. H. H. Huang, F. Q. Yan, Y. M. Kek "Synthesis, Characterization, and Nonlinear Optical Properties of Copper Nanoparticles" *Langmuir*, 13, 172-175, 1997.
59. Hideyuki Inaiye, Koichiro Tanaka "Femtosecond optical Kerr effect in Gold Nanopartical system", *Jpn. J. Appl. Phys*. Vol-37, L1520-1522, 1988.
60. Seong-Min Ma1, JaeTae Seo1, WanJoong Kim "Cubic Nonlinear Optical Properties of Ag Nanoparticles and Ag/Au Coreshells", *Journal of Physics: Conference Series* 109 (2008).
61. Found at internet address: Thermal analysis of Rubber. http://www2.shimadzu.com/applications/thermal/t115.pdf
62. M. Thakur and B.S. Elman, J. Chem. Phys., 90 (1989) 2042
63. Ernesto L Rodriguez, Frank Filisko Department of Materials and Metallurgical Engineering, Macromolecular Research Center. " Thermal effects in Styrene-butadiene rubber at high hydrostatics pressure" 1986
64. Treloar, "The physics of Rubber Elasticity"
65. I. Franta," Elastomers and Rubber compounds".

66. Found at internet address: http://www.sigmaaldrich.com/catalog/product/aldrich/182141?lang=en&region=US&cm_sp=Customer_Favorites-_-Detail_Page-_-Text-182141
67. J. Titus and M. Thakur, Appl. Phys. Lett., 90 (2007) 121111.
68. Index of Refraction - from Eric Weisstein's World of Physics" Wolfram Research. Found at internet address: http://scienceworld.wolfram.com/physics/
69. R. Swamy, H. Rajagopalan, P. Vippa, M. Thakur, A. Sen, Solid State Comm., 143 (2007)
70. Found at internet address: http://www.turnerdesigns.com/t2/doc/appnotes/S-0075.pdf
71. Mark S. M. Alger, Polymer Science Dictionary
72. 'FTIR spectra and mechanical strength analysis of some selected rubber derivatives' S. Gunasekaran, R.K. Natarajan, A. Kala
73. N. Vasanthan and A. E. Tonelli, "FTIR investigation of the inclusion compound formed between trans-1,4-polyisoprene and urea", *Polymer,* Vol. 36 No. 25, pp. 4887-4889, 1995.
74. Arthur E. Wooward, N. Vasanthan, and Joseph P. Corrigan, "Infra red spectroscopic investigation of bulk crystallized trans-1,4-polyisoprene", *Polymer*, Vol.34 No.11, 1993.
75. V. Arjunan a, S. Subramanian a, S. Mohan "Fourier transform infrared and Raman spectral analysis of trans-1,4-polyisoprene" *Spectrochimica Acta Part A* 57, 2547–2554, 2001.

76. G. Nimitz, A. Enders, P. Marquardt, R. Pelster and B. Wessling, Synth. Met., 45 (1991)197.

77. K. Uchida, S. Kaneko, S. Omi, C. Hata, H. Tanji, Y. Asahara, and A. J. Ikushima, J. Opt. Soc. Am. B, 11 (7) (1994) 1236.

78. "Semiconductor and Metal Nanocrystals", ed. V.I. Klimov, Marcel Dekker, New York, 2004, pp.422-431.

79. Bu-Xuan Wang, Le-Ping Zhou, Xiao-Feng Peng, "Surface and Size Effects on the Specific HeatCapacity of Nanoparticles" *International Journal of Thermophysics*, Vol. 27, No. 1, 139-151, (2006)

80. J. Rupp, R. Birringer, " Enhanced Specific Heat Capacity (C_p) measurements (150-300K) of nanometer-sized crystalline materials", *Physical Review B* Vol. 36, 1987

81. Differential Scanning Calorimetry, second and third order transitions in polymers http://www.colby.edu/chemistry/PChem/lab/DiffScanningCal.pdf

82. SII Nanotechnology, "Specific Heat Capacity Measurement Using DSC-I" *Japan* (1981)

83. Huafeng Shao, Baochen Huang, Wei Yao, Haixia Li, "Synthesis and characterization of low relative molecular weight trans-1,4-poly(isoprene)" *Journal of Applied Polymer Science*, Vol. 107, Issue 6, pages 3734–3738, 2008

84. Edward G. Lovering, David C. Wooden, "Equilibrium Melting points of the Low melting and High melting Crystalline Forms of trans-1,4-polyisoprene " *Journal of Polymer Science Part A*-2, Vol.9, 175-179, 1971

85. An-Long Li, Xiao-Yan Wang, Hui Liang, Jiang Lu "Controlled Radical co-polymerization β-Pinene and n-butyl acrylate" 2006

86. U.S. Census Bureau, International Data Base, 2008 First Update

87. History: Energy Information Administration (EIA), International Energy Annual 2004 (May-July 2006)

88. Projections: EIA, System for the Analysis of Global Energy Markets (2007)

89. World Consumption of Primary Energy by Energy Type and Selected Country Groups, 1980-2004. Energy Information Administration, U.S. Department of Energy (July 31, 2006). Retrieved on 2007-01-20.

90. Kearns D. R, Calvin M, J. Chem. Phys., 29, (1958), pp. 950

91. Paul A. Lane and Zakya H. Kafafi, Solid-state Organic Photovoltaic: A review of Molecular and Polymeric Devices, Naval Research Laboratory, Washington, D.C.,USA

92. Glenis S., Horowitz G., Tourillon G., Garnier, F., Thin solid Films, 111(2), (1984),pp. 93-103

93. Fang Y., Chen S. A., Chu M. L., Synth. Met., 52(3), (1992), pp. 261-272

94. Horowitz G., Garnier F., Sol. Energy Mater., 13(1), (1986), pp. 47-55.

95. A Palthi , A Narayanan , M Thakur "Photovoltaic Effect in a Composite involving the Nonconjugated Conductive Polymer, Poly(ß-pinene) and C_{60} "